

Ph.D. Dissertation



International Doctoral School in Information
and Communication Technology
DISI - University of Trento

DISTRIBUTED MONITORING FOR USER
LOCALIZATION AND PROFILING IN SMART
ENVIRONMENT

Giarola Enrico

Advisor:
Paolo Rocca
University of Trento
Tutor:
Federico Viani
University of Trento

February 2018

To my wife, my parents and my family, for their continuous and kind participation during this travel.

A special thanks to all friends and colleagues of the ELEDIA Research Center.

Abstract

The study of the next-generation distributed systems for distributed monitoring and user localization in smart environment is treated in this thesis. In the last years, a growing amount of attention has been focused on the adoption of Wireless Sensor Networks (WSN) as a scalable and flexible backbone to implement innovative services in smart environments, like smart building and smart cities. In this framework, this thesis will describe heterogeneous solutions to improve the supervision, control, monitoring, and management of public and private spaces. All these systems exploit the wireless communication and sensing in combination with smart methodologies to provide advanced services to the end user in many application fields, from environmental monitoring to energy management in smart districts or private and public buildings, up to road security and indoor occupancy for management and security reason. The data acquired by the WSN technology are used as input of customized strategies and algorithms developed for the real-time processing, fast analysis and result visualization.

Keywords

Wireless Sensor Network, Smart Environment, Distributed Monitoring, Power Metering, Occupation Estimation

Published Conference Papers

- [C1] G. Oliveri, E. Giarola, L. Manica, P. Rocca, L. Gandini, G. Ruscitti, and A. Massa, "An innovative planning tool for 3G wireless cellular networks," *PIERS 2011 in Suzhou*, Suzhou, China, September 12-16, 2011.
- [C2] F. Viani, M. Salucci, F. Robol, E. Giarola, and A. Massa, "WSNs as enabling tool for next generation smart systems," *Atti XIX Riunione Nazionale di Elettromagnetismo (XIX RiNEm)*, Roma, pp. 393-396, 10-14 Settembre 2012.
- [C3] F. Viani, F. Robol, M. Salucci, E. Giarola, S. De Vigili, M. Rocca, F. Boldrini, G. Benedetti, and A. Massa, "WSN-based early alert system for preventing wildlife-vehicle collisions in Alps regions - From the laboratory test to the real-world implementation," *EuCAP 2013*, Gothenburg, Sweden, pp. 1857-1860, April 8-12, 2013.
- [C4] G. Menduni, F. Viani, F. Robol, E. Giarola, A. Polo, G. Oliveri, P. Rocca, and A. Massa, "A WSN-based architecture for the E-Museum - The experience at "Sala dei 500" in Palazzo Vecchio (Florence)," *Proc. 2013 IEEE AP-S International Symposium*, Lake Buena Vista, Florida, USA, pp. 1114-1115, July 7-12, 2013.
- [C5] F. Viani, F. Robol, A. Polo, E. Giarola, and A. Massa, "Localization strategies in WSNs as applied to landslide monitoring," *2013 American Geophysical Union Fall Meeting*, San Francisco, USA, p. A5, December 9-13, 2013 (Invited paper; Session title: "New technologies in landslide monitoring and risk management" - A. Pasuto and L. Schenato).
- [C6] F. Viani, F. Robol, E. Giarola, G. Benedetti, S. Devigili, and A. Massa, "Advances in wildlife road-crossing early-alert system: new architecture and experimental validation", *8th European Conference on Antennas and Propagation (EuCAP 2014)*, The Hague, The Netherlands, pp. 3457-3461, April 6-11, 2014.

-
- [C7] A. Polo, F. Viani, E. Giarola, G. Oliveri, P. Rocca, and A. Massa, "Semantic wireless localization enabling advanced services in museums", *8th European Conference on Antennas and Propagation (EUCAP 2014)*, The Hague, The Netherlands, pp. 443-446, April 6-11, 2014.
- [C8] F. Viani, E. Giarola, A. Polo, G. Vannuccini, L. Longo, and A. Massa, "Decision support system for museum management through distributed wireless sensing," *MWF2014: Museums and the Web*, Florence, Italy, February 19-21, 2014.
- [C9] F. Viani, A. Polo, E. Giarola, F. Robol, P. Rocca, P. Garofalo, S. De Vigili, G. Benedetti, L. Zappini, A. Zorer, S. Marchesi, and A. Massa, "Semantic wireless localization for innovative indoor/outdoor services," *Proc. 2014 IEEE AP-S International Symposium and USNC-URSI Radio Science Meeting*, Memphis, Tennessee, USA, pp. 402-403, July 6-12, 2014.
- [C10] E. Giarola, S. Marchesi, A. Polo, F. Robol, F. Viani, L. Zappini, A. Zorer, and A. Massa, "Innovative wireless solutions for smart cities," *Atti XX Riunione Nazionale di Elettromagnetismo (XX RiNEm)*, Padova, pp. 385-388, 15-18 Settembre 2014.
- [C11] F. Viani, E. Giarola, F. Robol, G. Oliveri, and A. Massa, "Distributed monitoring for energy consumption optimization in smart buildings," *Proc. 2014 IEEE Antenna Conference on Antenna Measurements and Applications (IEEE CAMA 2014)*, Antibes Juan-les-Pins, France, pp. 1-3, November 16-19, 2014.
- [C12] F. Viani, F. Robol, E. Giarola, A. Polo, A. Toscano, and A. Massa, "Wireless monitoring of heterogeneous parameters in complex museum scenario," *Proc. 2014 IEEE Antenna Conference on Antenna Measurements and Applications (IEEE CAMA 2014)*, Antibes Juan-les-Pins, France, pp. 1-3, November 16-19, 2014.
- [C13] F. Viani, E. Giarola, F. Robol, A. Polo, A. Lazzareschi, T. Moriyama, and A. Massa, "Passive wireless localization strategies for security in large indoor areas," *Proc. 2014 IEEE Antenna Conference on Antenna Measurements and Applications (IEEE CAMA 2014)*, Antibes Juan-les-Pins, France, pp. 1-3, November 16-19, 2014.
- [C14] F. Viani, F. Robol, E. Giarola, P. Rocca, G. Oliveri, and A. Massa, "Passive imaging strategies for real-time tracking of non-cooperative targets in security applications," *9th European Conference on Antennas and Propagation (EUCAP 2015)*, Lisbon, Portugal, pp. 1-4, April 12-17, 2015 (Invited paper; Session title: "Wave-based sensing

-
- and imaging for security applications" à J. Martinez and C. Rappaport).
- [C15] F. Viani, E. Giarola, P. Rocca, G. Oliveri, and A. Massa, "Wireless coverage optimization for robotic swarm in emergency scenario," *Proc. 2015 IEEE AP-S International Symposium and USNC-URSI Radio Science Meeting*, Vancouver, BC, Canada, pp. 276-277, July 19-25, 2015.
- [C16] F. Robol, F. Viani, A. Polo, E. Giarola, P. Garofalo, C. Zambiasi, and A. Massa, "Opportunistic crowd sensing in WiFi-enabled indoor areas," *Proc. 2015 IEEE AP-S International Symposium and USNC-URSI Radio Science Meeting*, Vancouver, BC, Canada, pp. 274-275, July 19-25, 2015.
- [C17] F. Robol, F. Viani, E. Giarola, and A. Massa, "Wireless sensors for distributed monitoring of energy-efficient smart buildings," *Proc. 2015 IEEE Mediterranean Microwave Symposium (MMS-2015)*, Lecce, Italy, pp. 1-4, November 30 à December 2, 2015.
- [C18] F. Viani, A. Polo, and E. Giarola, "Exploiting EM simulation modelling for wireless indoor localization," *10th European Conference on Antennas and Propagation (EUCAP 2016)*, Davos, Switzerland, pp. 1-4, April 11-15, 2016.
- [C19] F. Viani, F. Robol, A. Polo, and E. Giarola, "Wildlife road-crossing monitoring system: Advances and test site validation," *10th European Conference on Antennas and Propagation (EUCAP 2016)*, Davos, Switzerland, pp. 1-4, April 11-15, 2016.
- [C20] H. Ahmadi, M. S. Dao, E. Giarola, A. Polo, F. Robol, F. Viani, and A. Massa, "Distributed wireless sensing, monitoring, and decision support: current activities @ ELEDIA Research Center," *Atti XXI Riunione Nazionale di Elettromagnetismo (XXI RiNEm)*, Parma, pp. 156-159, 12-14 Settembre 2016.
- [C21] F. Viani, A. Polo, F. Robol, A. Ferro, and E. Giarola, "Experimental validation of a wireless distributed system for smart public lighting management," *Proc. 2016 IEEE International Smart Cities Conference (ISC2)*, Trento, Italy, pp. 1-6, September 12-15, 2016.
- [C22] F. Viani, A. Polo, E. Giarola, G. Benedetti, S. Zanetti, and F. Robol, "Performance assessment of a smart road management system for the wireless detection of wildlife road-crossing," *Proc. 2016 IEEE International Smart Cities Conferenocce (ISC2)*, Trento, Italy, pp. 1-6, September 12-15, 2016.

-
- [C23] F. Viani, A. Polo, E. Giarola, M. Salucci, and A. Massa, “Principal component analysis of CSI for the robust wireless detection of passive targets,” *2017 International Applied Computational Electromagnetics Society Symposium, (ACES 2017)*, Firenze, Italy, pp. 1-2, March 26-30, 2017 (Invited paper; Special Session title: “Electromagnetic Techniques for the Internet of Things”, A. Costanzo and P. Nepa).

Published Journals Papers

- [R1] T. Moriyama, F. Viani, M. Salucci, F. Robol, and E. Giarola, "Planar multiband antenna for 3G/4G advanced wireless services," *IEICE Electronics Express*, vol. 11, no. 17, pp. 20140570(1-10), 10 September 2014.
- [R2] T. Moriyama, E. Giarola, M. Salucci, and G. Oliveri, "On the radiation properties of ADS-thinned dipole arrays," *IEICE Electronics Express*, vol. 11, no. 16, pp. 20140578(1-12), August 2014.
- [R3] F. Viani, A. Polo, M. Donelli, and E. Giarola, "A relocable and resilient distributed measurement system for electromagnetic exposure assessment," *IEEE Sensors Journal*, vol. 16, no. 11, pp. 4595-4604, June 2016.
- [R4] F. Viani, A. Polo, P. Garofalo, N. Anselmi, M. Salucci, and E. Giarola, "Evolutionary optimization applied to wireless smart lighting in energy-efficient museums," *IEEE Sensors Journal*, vol. 17, no. 5, pp. 1213-1214, March 2017.

Contents

1	Introduction	1
2	System Architecture	5
2.1	Wireless Sensor Network	5
2.1.1	The Architecture of a WSN	6
2.2	System Prototypes	10
2.2.1	Wildlife Road-Crossing Event Detection System	10
2.2.2	Wireless Distributed System for Smart Public Lighting Management	15
3	Distributed Monitoring for Energy Consumption Optimization	27
3.1	Distributed Monitoring for Energy Consumption Optimization in Smart Building	29
3.1.1	System Architecture	30
3.1.2	Control Strategy	31
3.1.3	Numerical and Experimental Results	34
3.2	Wireless Smart Lighting in Energy-Efficient Museums	45
3.2.1	Wireless Architecture	45
3.2.2	Control Strategy (Particle Swarm Optimizer)	46
3.2.3	Experimental Validation	50
4	Opportunistic Occupancy Estimation System for Museum Environments	55
4.1	System Architecture	57
4.2	Control Strategy	59
4.2.1	Support Vector Machine	61
4.3	Experimental Validation and Results	66
4.3.1	WSN Node Prototype	66
4.3.2	Deployment in a Real Museum Environment	68
4.3.3	Occupancy Estimation	73
5	Conclusions	75
5.1	Conclusions and Future Developments	76

CONTENTS

List of Tables

2.1	Number of Monitored Lamps.	21
3.1	PAR values after the CP Optimizations.	38
3.2	Time-Slot for each user in “ideal” condition.	39
3.3	Time-Slot for each user in “real” condition.	40
3.4	Time-Slot for each user in “complex” condition.	41
3.5	PAR values after the CP Optimizations varying the time slot conditions.	42

LIST OF TABLES

List of Figures

2.1	Architecture of a wireless sensor node.	7
2.2	Network architectures in a WSN: (a) “star” topology-nodes communicates only with the gateway, (b) “mesh” topology-data transmission is performed through node-to-node communications, and (c) “cluster” topology-the network is subdivided into clusters.	9
2.3	Experimental test-site: (a) wildlife road-crossing and (b) security area of the WSN-based system.	12
2.4	WSN node installed on road delimiters of the experimental test-site.	13
2.5	Event detection at the experimental test-site: (a) actual road-crossing event and (b) related measured data.	14
2.6	Statistical analysis of the system detection capability.	14
2.7	WSN node installed in the streetlight pole.	16
2.8	WSN-based smart lighting system architecture.	17
2.9	Internal (a) and external (b) antenna installation.	18
2.10	Test sites in dense urban area (a) and in rural area (b).	19
2.11	Comparison of power consumption profiles <i>pre</i> and <i>post</i> installation.	22
2.12	Power consumption profiles of the the $I_8 = 51$ controlled nodes.	23
2.13	Dimming profiles of the the $I_8 = 51$ controlled nodes.	23
2.14	Brightness level measured by the lux meter.	24
2.15	Energy saving during the experimental campaign.	24
3.1	Wireless architecture in smart home test site.	31
3.2	System architecture for energy monitoring and optimization.	33
3.3	Player 1 - appliances schedule before and after optimization.	35
3.4	Original versus optimized energy profiles.	36
3.5	Performances of the GT-based approach varying the number of users P : (a) $P = 2$, (b) $P = 4$, (c) $P = 6$, (d) $P = 8$ and (e) $P = 10$	37
3.6	Performances of the GT-based approach varying the time slot conditions.	42
3.7	Experimental setup for wireless power metering and control.	43
3.8	Graphical interface for data visualization and management.	44

LIST OF FIGURES

3.9	WSAN architecture for smart lighting in museums.	46
3.10	Particle Swarm Optimizer: (a) Bees searching a field for the location of the most flowers (b) All the bees swarm around the best location.	47
3.11	Particle swarm optimizer: flowchart.	48
3.12	Devices used in the experimental validation: (a) TI SensorTag, (b) Mi-Light dimmable lamps.	51
3.13	Test-case 1: (a) Fitness function evolution, (b) light intensity, (c) power consumption and (d) dimming profiles of the smart actuators in the regions of interest.	52
3.14	Test-case 2: (a) Fitness function evolution, (b) light intensity, (c) power consumption and (d) dimming profiles of the smart actuators in the regions of interest.	53
3.15	Light intensity (a), power consumption in the regions of interest (b), and optimal dimming profiles of the smart actuators (c).	54
4.1	Hybrid WSN architecture for complex museum monitoring.	58
4.2	WSN deployment in a museum.	59
4.3	Vertical distributions of (a) the temperature profile $\alpha(h, t)$, and (b) the humidity profile $\beta(h, t)$	60
4.4	Non-linear mapping of the input space to the feature space.	63
4.5	Prototype of the WSN sensor node.	67
4.6	EMuseum Web Tool.	69
4.7	Network Installation inside the “Sala dei 500”.	70
4.8	Sensing layers inside the “Sala dei 500”.	71
4.9	WSN Node Diagnostic Information.	72
4.10	WSN Node Historic Data.	72
4.11	Derivatives of daily vertical profiles of (a) the temperature, and (b) the humidity.	73
4.12	Actual and estimated indoor occupancy.	74

Chapter 1

Introduction

In the last decade, the vision of widespread computing as an emerging model for the next-generation smart systems [1] has become more and more relevant thanks to the increase of computing and communication capabilities as well as in interactions with end users. The miniaturization of portable and multi-features devices has contributed to the diffusion of terminals able to communicate in an active way with distributed networks for communications and information acquisition. In this framework, the Wireless Sensor Networks (WSNs) [2, 3] have been investigated as enabling technology for next generation intelligent networks and services that can satisfy the arising user needs. One of the main characteristic of WSNs devoted to smart systems is that, to overcome the limited capabilities of each single sensor node, cooperative schemes throughout the whole network can be implemented to enable the solution of even complex tasks [6]. Moreover, heterogeneous functionalities can coexist thanks to the multi-sensor characteristic of each node, by enabling multiple applications within the same hardware backbone. For all the well-known features of the WSN technology, has been investigated the design of a cross-layer architecture for the implementation of smart systems where heterogeneous and multiple functionalities can be integrated for the solution of different user needs in smart environments.

For this reason this work deals the WSNs for the distributed monitoring of heterogeneous parameters and its advanced application in two principal smart environments: the Smart Cities and the Smart Building.

The concept of Smart Cities can be applied to different outdoor applicative scenarios; in this work road security and public light management systems are proposed. In the context of road security a system for the monitoring of roadsides for the real-time detection of wildlife road-crossing events has been realized using wireless sensors equipped with low-cost Doppler radars. This solution aspires to alert the approaching drivers to prevent the risk of wildlife-vehicle collisions. The main challenge of the system is to process the acquired radar signals in real-time to activate the road signs only when actual events occur, in order to reduce the users habit-forming to fixed signs. On the other hand, in the context of pub-

lic light managements, a system for the smart management of public lighting is proposed. This system is aimed at reducing the power consumptions of the street lamps. The distributed and adaptive control of the dimming profiles has been investigated taking in consideration the time-varying environmental conditions. The presented system is able to control each single lamp thanks to the integration of smart wireless devices in the existing light poles. Both these systems have been installed in experimental sites, in order to test and evaluate their performances. The road security system has been deployed along a real stretch of road, in Cavalese (Trento), in the north of Italy, while the public lighting management system has been installed in different areas of the city of Trento, in cooperation with the municipality of Trento, which is responsible for the control and maintenance of the public lighting. The advantages and the limitations of the proposed solutions will be experimentally assessed and their performances will be evaluated.

Moreover, the smart monitoring of indoor areas (Smart Building) with wireless sensors will be analyzed, by presenting systems developed in two different application fields: consumption optimization in smart environment and opportunistic occupancy estimation in smart museum.

Nowadays, efficient energy saving strategies and solutions are very important to increase user awareness of energy resources management in social and economic aspects. The traditional power grid needs new monitoring and control tools for the optimal management of producers and consumers through adaptive energy distribution schemes. The issue of energy consumption reduction can be addressed at different scales, ranging from the management of single home appliances up to building, district, and city level. In this work, a wireless system architecture for the distributed monitoring and intelligent supervision of energy consumptions in smart home is proposed. The energy information related to a multi-user scenario are acquired by distributed wireless sensors and processed by a decision-making support tool aimed at the adaptive optimization of user's energy-habits and successive energy cost reduction. In a smart museum environment an intelligent lighting system control is proposed. It treats multiple and competing targets, such as the energy saving as well as the quality of the visitor experience. In this context, to adaptively control the light intensity starting from the real-time measurement of the energy consumption and brightness conditions, an evolutionary optimization strategy is proposed. The system is implemented using low-cost wireless devices and it has been experimentally validated in a real indoor test site.

In a particular environment like a museum, beyond the control of a lighting system, the artwork conservation is one of the most important purposes to reach. For this reason, an environmental monitoring system designed for museum scenarios is proposed in this work. Nowadays environmental monitoring systems are largely employed in order to measure parameters for artworks conservation and to control exhibitions in order to avoid and prevent critical events,

as for example damages or theft. In this context the WSN technology allows the non-invasive integration of such monitoring functionalities in complex museum scenarios, that can be hosted also in historic buildings. The proposed system deals with the problem of monitoring multiple physical parameters of interest for museum curators, exploiting the advantages of a pervasive, cooperative, and flexible WSN architecture. Moreover, a scalable and low-cost solution for occupancy estimation in museums is here proposed by exploiting in an opportunistic way the wireless architectures already deployed for artworks conservation purposes. The information about the presence and the distribution of the visitors is produced throughout the analysis of the environmental parameters acquired by the proposed monitoring system. Indeed, the relationships between museum fruition and environmental indexes are deduced by a learning-by-example technique. An experimental application of this system in a real museum site is also presented and discussed to give a proof of the reliability and efficacy of the proposed approach.

Thesis outline

The thesis is organized as follows. Firstly, the general architecture of all the systems is discussed, by analyzing the Wireless Sensor Network technology in Chapter 2, with some example of distributed monitoring systems developed in the smart city context. Then, the problem of distributed monitoring for energy consumption optimization in smart building is presented in Chapter 3, with a detailed description of two systems for consumption optimization: a Distributed Monitoring for Energy Consumption Optimization in Smart Building and Wireless Smart Lighting for Energy-Efficient Museums, analyzing the technological and methodological features of each system. In Chapter 4 the specific museum environmental monitoring problem is analyzed and a monitoring system for this type of environment is proposed. In this Chapter an opportunistic occupancy estimation system will be proposed too. Then the final conclusions are drawn in Chapter 5.

Chapter 2

System Architecture

In this Chapter, the Wireless Sensor Network (WSN) technology is presented. This technology is used for the distributed monitoring of heterogeneous parameters and is characterized by small, low-cost, and autonomous devices that collect data about physical quantities in a distributed and pervasive fashion. This technology has been applied to many systems in order to remotely control parameters and actuate actions when these parameters assume particular values, by notifying a message to an operator or performing actions that modify them. After the introduction to this technology, two WSN prototypes developed in the context of Smart Cities during my Ph.D. at ELEDIA Research center will be presented.

2.1 Wireless Sensor Network

The Wireless Sensor Network (WSN), is a technology based on a network of tiny, low-cost, low-power, and autonomous devices (called nodes) that use sensors to monitor physical quantities [4, 5] in a cooperative way. Recently, WSNs have achieved much attention in many research areas for their ability to enhance the interactions between environment, humans, and machines.

If we compare the WSN to traditional communication networks, they do not have any physical infrastructure that restricts their topology. These networks combine simple wireless communication techniques, minimal computation facilities, and the sensing of the physical environment into a new form of network [6]. Moreover, low-cost hardware allows the pervasive and dense deployment of many nodes in the physical environment, with a scalability property provided by the flexible network architecture. Unlike other large and medium-scale observation technologies, WSNs not only sense the environment but also provide some interactions by exploiting the functionality of a set of so-called actuator nodes. These systems are known as Wireless Sensor Actuators Network (WSAN) [7], and are characterized by sensors that collect information about the physical world and transmit them to some controllers. Finally, the actuators will perform suitable actions to influence the physical behavior of the system under test. [3]

2.1.1 The Architecture of a WSN

A WSN typically consists of a network of sensor nodes, that measure the monitored parameters, and a gateway (called also sink node), that collects these parameters and provides the connection with the external world (i.e., through Internet). Each sensor node is typically equipped with: a radio transceiver or other wireless communications device, a small micro-controller, and an energy source. The size of the single unit can vary from about ten centimeters to several millimeters, but future implementations will probably be characterized by smaller size, thus allowing a more dense deployment in the physical environment [8]. In order to describe a typical WSN, we will focus mainly on the characteristics of a sensor node and on the network architectures. For a more detailed overview about the architectures and technologies for the Wireless Sensor Networks, the interested reader can refer to [6], [5] and the references cited therein. [3]

2.1.1.1 Wireless Sensor Node

A wireless sensor node consists of a processing unit with a storage device, one or multiple sensors, a radio unit, and a power unit, as represented in Fig. 2.1.

Each subsystem of these nodes is designed in order to minimize the energy consumption, because the WSN typically operates for enough long time periods in harsh environments. For the same reason, the processing unit is composed by a small processor with limited computational power. This processor aims at the careful management of the limited power resources (e.g., by activating the sensing and radio units only when needed) and takes care of the reception, transmission, storage and processing of data. As an example, the TinyNode 584 is equipped with a Texas Instruments MSP430 micro-controller [9]. This micro-controller features low power mode and it is optimized to achieve extended battery life in measurement applications. Such a micro-controller is characterized by a 16-bit RISC CPU with 16-bit registers, 10 kB of RAM, and 48 kB of flash memory. The digitally controlled oscillator (DCO) allows wake-up from low-power mode to active mode in less than $6\mu\text{s}$ and may operate up to 8 MHz. The MSP430 has a current consumption of $0.2\mu\text{A}$ in the sleep mode and 2.5 mA in the active mode, in typical operating conditions.

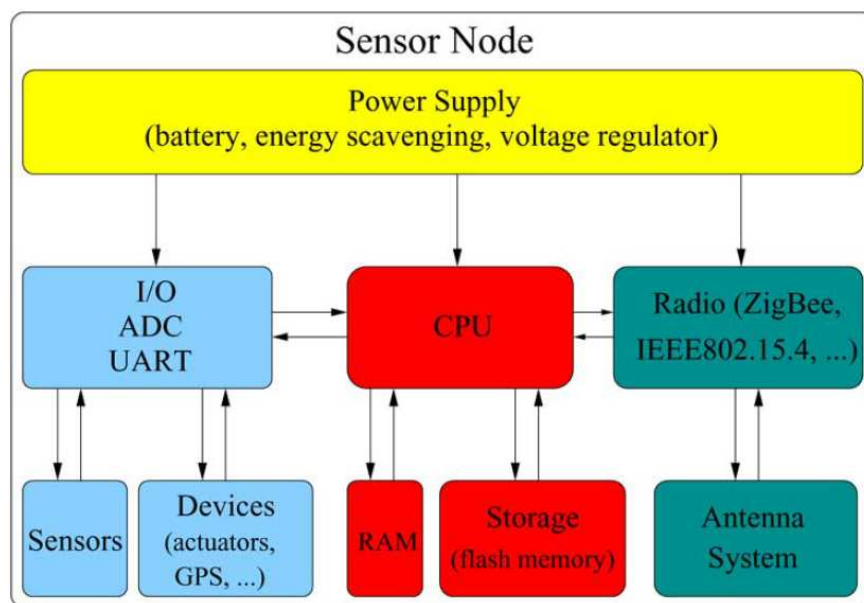


Figure 2.1: Architecture of a wireless sensor node.

Regarding the sensing unit, it consists of one or multiple sensors that convert a physical quantity into an electric signal, that can be processed and stored in a memory. For this device a typical sensing tasks can be the measurement of temperature, light, vibration, sound, and radiation. Recently, innovative sensors have appeared thanks to the exploitation of micro electro-mechanical systems (MEMS) [10].

The data exchange is the most expending operation for a WSN node. The authors of [11] state that the power required to transmit one bit of information for a 100 m distance is equivalent to the amount of power needed for the implementation of the 3000 instructions calculation. For this reason, the radio transceiver is probably the most critical device in the design of a sensor node. Since node-to-node communications are carried out mostly in a short range, power consumptions related to transmission and reception are on average similar [6]. Data exchange typically requires a start-up phase after the activation of the radio unit, mostly related to the lock time of the phase-locked loop (PLL). During this phase, which may take a time similar to the duration of the transmission phase, a non-negligible amount of power is wasted. It may be convenient to switch off the radio unit after data transmission in the case sporadic sensing, whereas start-up time could be responsible for wasting power in constant event monitoring. Regarding to the power consumption, the radio module of the TinyNode 584 requires 62 mA in the transmit mode (at the maximum power), 14 mA in the receive mode, and 4 μ A in sleep mode. Concerning the speed of data exchange, sensor nodes are characterized by data rates up to 250 kbps in

the 2.4 GHz ISM band when using IEEE 802.15.4 protocol or up to 40 kbps within the 868 MHz ISM band. Anyway, data rates depend on the antenna gain, on the nodes transmission power, on the background noise, and on the value of the Signal-to-Interference-plus-Noise Ratio (SINR) at receiver.

For these reasons, the power source has to be chosen taking into consideration a mathematical model for radio power consumption [12]. Usually, in many application environment, power sources cannot be recharged or replaced and consequently their design can define the sensor node and network lifetime. As an example, the sensor node TinyNode 584 with a subsoil thermometer and five soil moisture sensors may require up to 120 mA at 6 V for about 2 s in the active mode and 80 μ A for the remaining duty cycle time. If the sampling rate is equal to 10 minutes and its power source is a 1.2 Ah battery, the lifetime of the unit is limited to three months. However, thanks to the use of an energy scavenging technology, such as a solar panel providing 250 mA at 7 V, the lifetime of the wireless node can be potentially extended to infinite (limited only by the maximum number of the battery charge/discharge cycles). Recently, thanks to the advances in nanotechnologies and MEMS, more effective energy scavenging (or harvesting) solutions have been developed in order to recharge the power source by means of the exploitation of the physical environment where the nodes are deployed [13]. Although this technologies can generally provide a limited amount of power, they appear to be compatible with WSN because of the low-cost and small size of each sensor node. [3]

2.1.1.2 Network Architecture

The power consumption of the sensor node can be influenced also by the network architecture.

As shown in Fig. 2.2, the simplest network architecture is the so-called “star” topology, where all nodes communicates only with the gateway. This configuration is used for simple scenarios, where the spatial density of the nodes is limited and the coverage of the gateway reaches all the sensor nodes of the network (e.g., when sensor nodes are in line-of-sight of the gateway). Moreover, the “star” topology is mainly used when nodes need only to transmit information to the gateway. Despite the architectural simplicity, this architecture involves an important drawback in terms of network reliability, because the gateway is a single point of failure and is usually characterized by a greater power consumption [12].

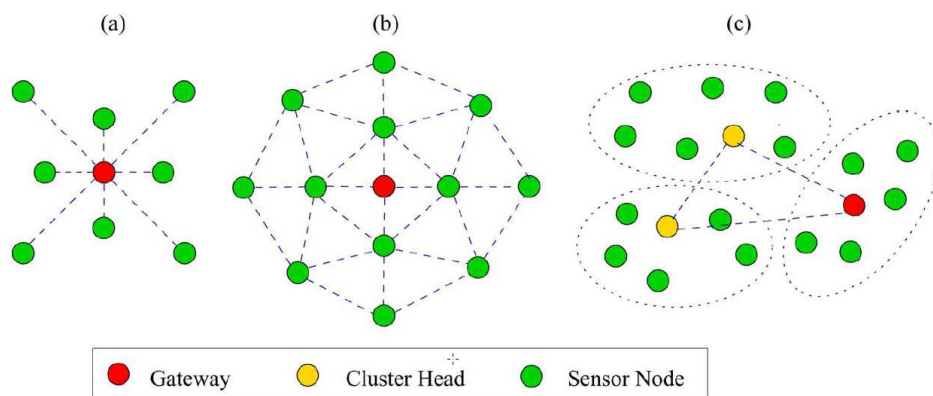


Figure 2.2: Network architectures in a WSN: (a) “star” topology-nodes communicates only with the gateway, (b) “mesh” topology-data transmission is performed through node-to-node communications, and (c) “cluster” topology-the network is subdivided into clusters.

A more effective solution to deal with complex scenarios consists in the use of “mesh” topologies, where data exchange is mainly carried out by means of node-to-node communications. This architecture is characterized by a uniform power consumption and provides a high degree of reconfigurability and scalability, but requires complex and computationally expensive routing algorithm in order to control data transmission [6], [14].

To manage the data transmission and optimize the power consumption, the sensor nodes can be organized using hybrid architectures where the entire network is subdivided into clusters coordinated by the “cluster heads” [12]. The “cluster head” selection and partitioning procedure are usually real-time and continuously performed, taking into account the network topology as well as the energy/signal level of each unit. [3]

2.2 System Prototypes

Nowadays, the smart city paradigm is attracting more and more attention of both researchers and industries, thanks to the enormous advantages that smart technologies and services can provide to citizens and public administrations [21]. Among the emerging topics, those related to security, surveillance, mobility, health, and energy have been mostly investigated because of the immediate and evident impact of innovative information communication technologies (ICT) as applied to smart city services [22].

In this Section will be proposed two systems related to this topic:

1. Road security: wildlife road-crossing event detection system;
2. Power management: wireless distributed system for smart public lighting management;

2.2.1 Wildlife Road-Crossing Event Detection System

Wildlife monitoring is attracting more and more attention during the last decade. Most of the studies are focused on the understanding of animal behavior, their physiology, socialization, and diffusion [17][18][19]. To this end, researchers have proposed many autonomous monitoring systems mainly based on wireless sensor network (WSN) infrastructures [2][3]. [15]

Here a low-cost and scalable wireless system for the prevention of wildlife-vehicles collisions is proposed. In particular, the nodes of a WSN have been customized with dedicated Doppler radars for the real-time detection of wildlife presence on the roadsides. The detection of such event triggers the adaptive alert notification to the approaching drivers (through smart light road signs).

A system prototype has been developed and deployed in a real test-site for the performance assessment in real operative conditions. Long-term testing has been performed to verify the robustness of the system in different seasons and weather conditions. The number of detected events has been statistically analyzed and compared with the ground truth acquired by means of a surveillance video recording system. [16]

2.2.1.1 System Architecture

The wireless network is composed by four node typologies according to the requested functionalities. The *gateway nodes* are dedicated to the data collection and forwarding to the control unit, that implements the processing and actuation strategies. The *anchor nodes* are devoted to the wireless network management through multihop architecture for coverage extension along the roadsides. The *actuator nodes* receive actuation commands when the control unit identifies a warning situation and turn on the light signals on the roadsides accordingly. Finally, the *sensing nodes* integrate the heterogeneous sensors for the detection of

moving animals. They are deployed on the roadsides and their position defines the security zone.

Each node is equipped with two Doppler radar modules (working frequency f_c , maximum coverage r_c , horizontal and vertical aperture $[h_c^o, v_c^o]$) with different orientations for improved detection in terms of horizontal aperture. The output signal of the radars is multiplexed in time (through an hardware switch) and a single output data stream $x_n(t_k)$, $n = 1, \dots, N$ being the node index, is sampled at time instants $t_k = t_0 + k\Delta t$, where t_0 is the boot time instant, $k = 1, \dots, K$ is the time sampling index (K being the maximum data samples that can be locally stored on the device memory), and Δt is a constant time interval a-priori defined according to the internal clock performance. Once $t_k = K\Delta t$, the older data are iteratively overwritten in order to have a local copy of the last newest K samples. A filtered version of the raw radar signal is successively processed by the customized filter function $\Phi(\bullet)$ has been introduced to discard the undesired movements (i.e., the too slow and the too quick target movements) and to enhance the radar signature of the desired target through signal rectification and amplification. The filtered signal is then analyzed by a calibrated hardware thresholder that provides in output the following binary behavior

$$\delta(t_k) = \begin{cases} 1 & \text{if } \hat{x}_n(t_k) \geq X_{th} \\ 0 & \text{if } \hat{x}_n(t_k) < X_{th} \end{cases} \quad (2.1)$$

where X_{th} is a calibrated triggering threshold .

If $\delta(t_k) = 1$ the WSN node reduces the sampling period Δt , activates the wireless transceiver, and transmits a scaled version of the filtered signal stored on the local memory. The transmission stops when $\delta(t_k) = 0$. Successively, the transceiver is shut down and Δt is restored to its default value. Transceiver modules complies with the IEEE 802.15.4 standard, operating at frequency $f_{tx} = 2.4GHz$ and equipped with monopole antenna for omnidirectional radiation pattern on the horizontal plane.

The transmitted data are received by the gateway node and forwarded to the remote control unit for additional real-time processing. In particular, temporal and spatial correlation of the received data are performed in order to estimate additional features of the wildlife movement and to evaluate offline statistics about the road risk-level.

In order to accurately assess the system performance for longterm test periods, the ground truth of the wildlife presence within the monitored road-sides has been also acquired. Toward this end, an infrared video-surveillance system has been installed in order to record the monitored road during the whole measurement campaign. The output of the verification system is a binary information related to the absence/presence of a target within a predefined area (along the road-sides) of the video recordings. Accordingly, the actual status of the scenario can be occupied if a target occupies the security area, or empty, otherwise. The comparison between the binary function and the ground truth provides a

2.2. SYSTEM PROTOTYPES

first performance evaluation in terms of false positive and false negative and detections. [16]

2.2.1.2 Experimental Validation

The wildlife monitoring system presented in this Sub-Section has been deployed along a real stretch of road, in the Alps region near Trento, in the north of Italy. The monitored test-site is 300m long [Fig. 2.3(a)]. $N = 21$ sensor nodes have been deployed along the test site, on the two sides of the road as shown in Fig. 2.3(b).

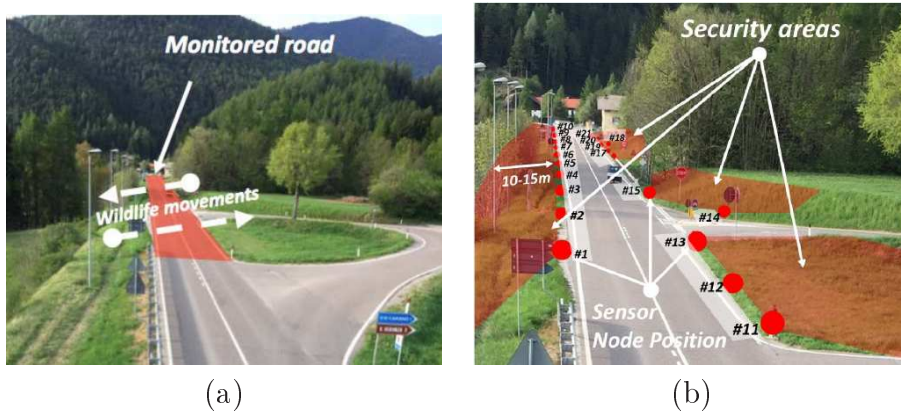


Figure 2.3: Experimental test-site: (a) wildlife road-crossing and (b) security area of the WSN-based system.

Two Doppler radar sensors, characterized by $F_c = 24GHz$, $r_c \equiv 15m$ and $[h_c^o, v_c^o] = [80^\circ, 32^\circ]$, have been integrated in each sensor node and properly oriented to obtain an horizontal aperture of about 160° . This allows the definition of the so-called security area [Fig. 2.3(b)]. The devices have been installed directly on the road delimiters, which are placed 20m far from each other (as stated by the Italian regulation).

The data-sampling rate is set to the default value of $\Delta t = 250ms$ [when $\delta(t_k) = 0$], and reduced to $\Delta t = 30ms$ [when $\delta(t_k) = 1$]. The transmission threshold has been set to $X_{th} = 30\%$.

In Fig. 2.4, a sensor node deployed in the experimental test-site is shown. As it can be noticed, two solar panels have been integrated on the lateral sides of the prototype, in order to extend the lifetime of the battery.



Figure 2.4: WSN node installed on road delimiters of the experimental test-site.

As a representative example of the experimental validation, a real event detected by the monitoring system is reported in Fig. 2.5. In particular, a snapshot of the ground truth acquired by the infrared verification system is shown in Fig. 2.5(a). The selected picture represents the actual position of the target moving towards the left side of the road (and entering in the radar coverage of the node $n = 2$). The corresponding scaled signal $\tilde{x}_2(t)$ compared with the ground truth $\xi(t)$ is reported in Fig. 2.5(b).

The comparison shows a good matching between the actual event and the measured signal, thus confirming the good capability of the system to detect the target. In particular, the sensor node has detected the target presence with a maximum delay of about 250ms, proportional to the sampling rate Δt .

Finally, regarding false positive and false negative analysis, Fig. 2.6 reports the number of actual daily events Ψ compared to the detected ones, during a 9-days measurement campaign. It may be noticed that 3 false-negative detections happened during the investigated period, thus leading the correct detection rate to 77%. False-negative detection are mainly related to target speed, which are filtered by the function $\Phi(\bullet)$ in case of too slow or too fast target movements. Further calibration procedures are under investigation to limit the false-negative detection and increase the system reliability. [16]

2.2. SYSTEM PROTOTYPES

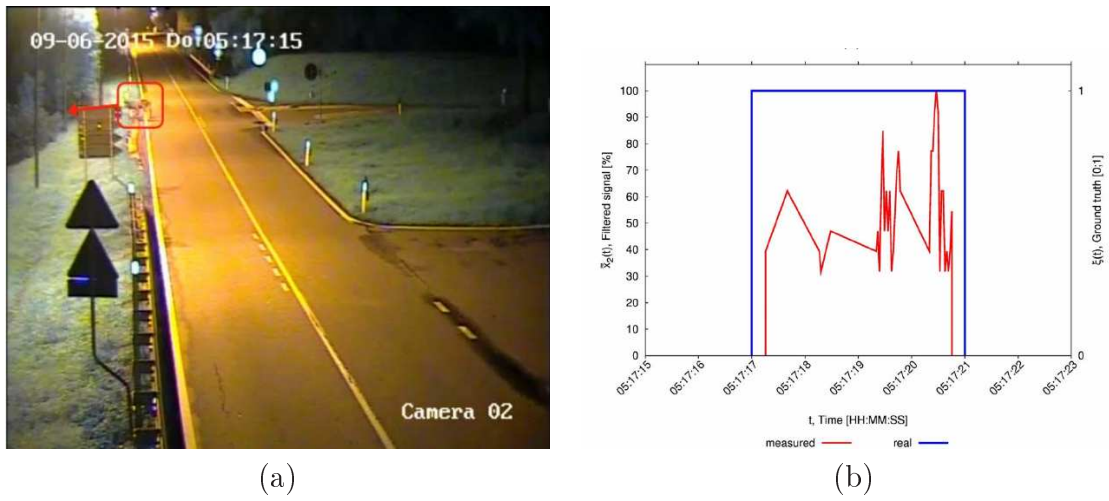


Figure 2.5: Event detection at the experimental test-site: (a) actual road-crossing event and (b) related measured data.

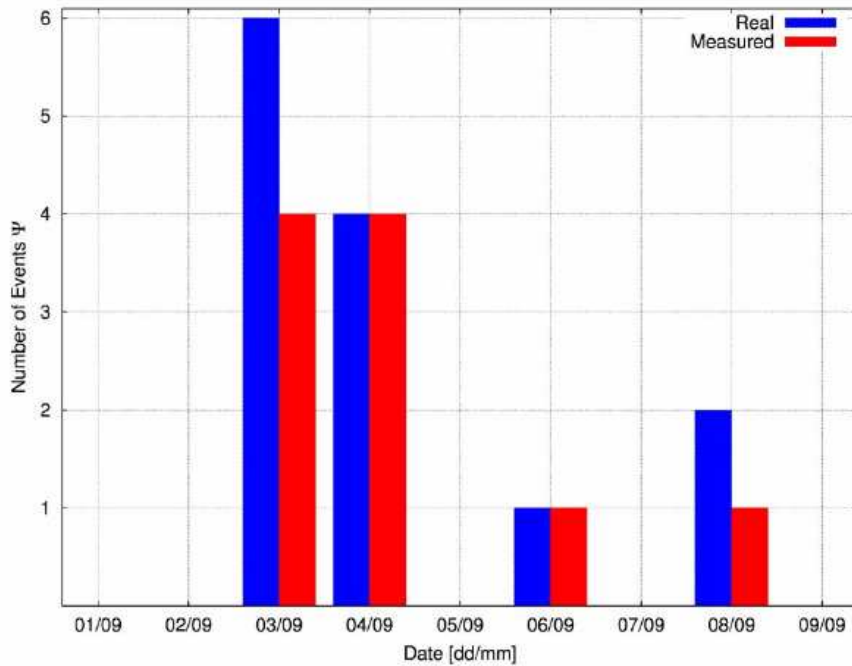


Figure 2.6: Statistical analysis of the system detection capability.

2.2.2 Wireless Distributed System for Smart Public Lighting Management

For energy-aware applications, the framework of smart grid is rapidly growing together with the upgrading of the electricity distribution and management. Advanced communication capabilities and improved control strategies are expected to affect all areas of the electric power system, from the generation to the distribution. Among the applicative fields related to the smart grid, the smart lighting is a representative example where the integration of new ICT tools is providing substantial energy saving [23][24]. Both indoor and outdoor lighting services have been improved by modern industrial solutions including efficient lamps, innovative electronic controls, soft-start systems, and smart actuation strategies [25]. Besides the improvement in the lighting devices, one of the main challenges to enable energy saving is the pervasive and adaptive control of the lighting network. Many methodological solutions have been proposed for in-building lighting management, where the energy saving has been obtained by dimming the lamps according to the indoor lighting conditions and to the user needs [39]. However, different strategies are required for the control of outdoor street lighting since other constraints exist. The high spatial extension, the huge number of lamps, the harsh environment conditions, the strict regulations on the quality of service, the high spatial variability of urban scenarios, the heterogeneity of the existing lighting networks, make the smart control of the public lighting a challenging task.

Even if different technological solutions are available, it has to be noticed that the costs for designing and deploying from scratch a new street lighting system is often too high for both private and public entities. Starting from this assumption, the inexpensive, scalable, and non-invasive solutions able to convert an existing system in a more energy-efficient one are preferred and considered the first step for the short-term cost saving. Accordingly, the wireless sensor network (WSN) technology represents a suitable alternative to enable the low-cost distributed monitoring and control. [20]

2.2.2.1 Application Requirements

The local public authority is responsible for the lighting management and one of the main concerns is to reduce the operation costs with minimum financial investments. This final objective determines the requirements to be satisfied by the proposed control system, which include:

1. the easy integration in the existing street lamps and cabinets (Fig. 2.7);
2. the absence of additional wiring or substitution of infrastructures and facilities.



Figure 2.7: WSN node installed in the streetlight pole.

At the same time, the proposed control system has to guarantee high robustness and reliability since the public lighting network offers a fundamental service to the citizens. The wireless network has to support hundreds of nodes and to guarantee reliable wireless links even in very complex urban environments. The adopted WSN nodes have to control the on/off sequences as well as the dimming profiles of the street lamps, to measure the power consumptions, to monitor the status of the lamps, and to handle the data exchange with the network. Moreover, besides the power consumption monitoring for energy saving, the system architecture may become an open backbone for other additional services in the framework of the smart cities and communities. To this end, both the hardware and software components are designed to manage additional sensors and features according to next generation services for the citizens. [20]

2.2.2.2 Wireless Network Features

The smart lighting system is based on a clustered mesh WSN composed by:

$$K = \sum_{n=1}^N I_n \quad (2.2)$$

wireless nodes, where $i^{(n)} = 1, \dots, I_n$, $n = 1, \dots, N$ are the nodes belonging to the clusters managed by the N coordinators, as pictorially shown in Fig. 2.8.

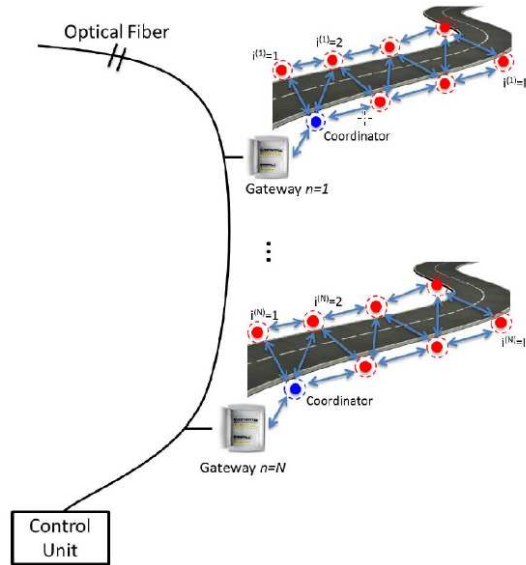


Figure 2.8: WSN-based smart lighting system architecture.

The coordinator nodes are interconnected to the gateway devices dedicated to the data forwarding from the wireless network toward the existing wired infrastructure. The spatial distribution of each cluster $n = 1, \dots, N$ depends on the geographical properties of the considered area as well as the electrical interconnection of the street lamps. As a basic rule, the lamps interconnected to the same electric line belong to the same cluster. However, the clusters can be reconfigured according to the time-varying characteristics of the urban environment and the consequent changes in the wireless signal propagation.

The WSN nodes have been placed within the structure of the light poles, close to the lamp and to the electronic ballast for easy access during the standard maintenance operations. The antenna can be internal or external according to the material properties (plastic or metallic) of the outer case, as represented in Fig. 2.9.

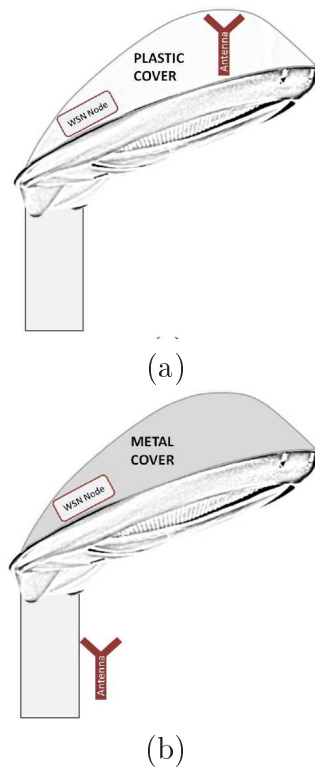


Figure 2.9: Internal (a) and external (b) antenna installation.

The robustness of the wireless network is guaranteed when each node is connected with more than one neighbor node, and the optimal network configuration is achieved when at least three neighbors are within the wireless coverage. Such an optimal configuration is easily satisfied in dense urban areas where many intersections among streets and alleys exist [Fig. 2.10(a)] but turns out to be more complex in rural areas where linear streets are more common [Fig. 2.10(b)]. In this configuration, the antenna positioning and the network electromagnetic planning have been carefully considered to guarantee a robust and stable wireless coverage. [20]

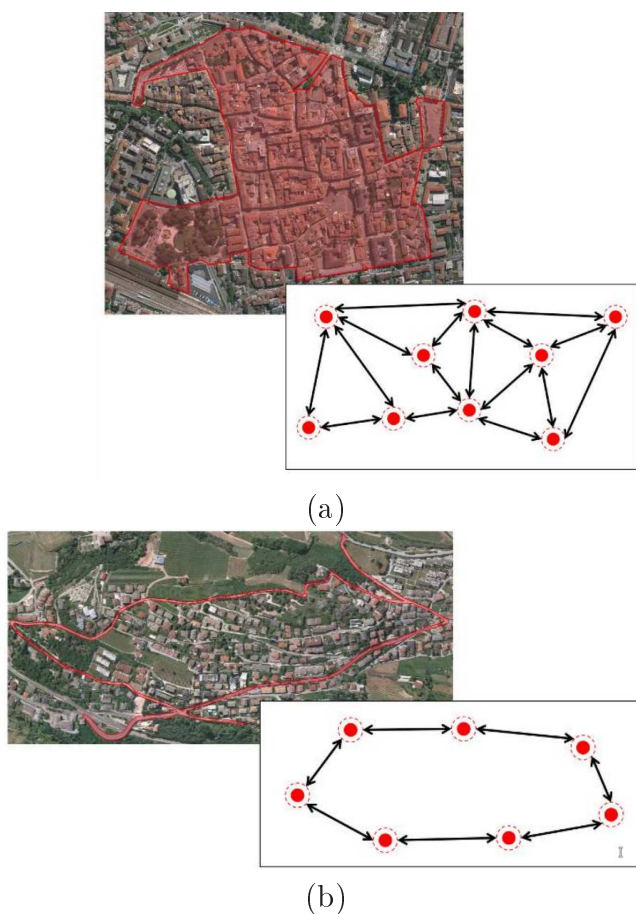


Figure 2.10: Test sites in dense urban area (a) and in rural area (b).

2.2.2.3 Node Control and Power Metering

Each WSN node handles the common street lighting operations, including the on/off and the dimming of the interconnected lamp. Moreover, the power consumption is measured in real-time by means of the on-board power metering subsystem. Respect to the standard metering solutions, which usually measure the total power consumption of the whole electric line, the power information of each individual lamp is acquired, thus enabling the analysis of the lamp diagnostic information, such as its voltage, the lamp ignition failure, or the lifetime statistics. The implemented onboard firmware provides different working modalities according to the status of the network. For example, if the control unit goes down because of system failure, the nodes automatically switch to the off-line mode and manage the lamps applying a predefined scheme in order to guarantee the minimum working capability and quality of service. The firmware of the nodes can be updated over the air sending simple commands from the main

control unit, avoiding the maintenance intervention directly on the streetlight poles. The remote control unit is interconnected to the WSN gateways through a wired network and hosts the software stack for data processing, storage, and visualization. The network managers can access the system from remote terminals through user-friendly tools and interfaces implemented at the application layer. Among the implemented features, the software enables the localization of all the monitored streetlights on a geographic information system (GIS) and all the information related to power consumption, diagnostics, sensor data, lamp information are easily accessible. The power dimming profiles can be configured for single or group of lamps providing high flexibility and timely update according to the requirements or to the environmental changes. The environmental brightness $\beta_m = [\beta_m(t); t = 1, \dots, T]$, $m = 1, \dots, M$, is measured at discrete time intervals $t = 1, \dots, T$ by a set of M lux meters deployed in multiple positions of the monitored streets and interconnected to the gateways. The environmental brightness conditions β_m , $m = 1, \dots, M$, and the energy consumptions of each single lamp E_k , $k = 1, \dots, K$, represent the input data of the control method, while the output is the set of dimming profiles $\underline{\delta} = \delta_k$, $k = 1, \dots, K$, where $\delta_k = [\delta_k(t); t = 1, \dots, T]$.

The objective of the control method is to identify the best profiles that minimize the cost function:

$$\Omega(\underline{\delta}) = a \left[\frac{1}{M} \sum_{m=1}^M \frac{\beta_m(\underline{\delta}) - \hat{\beta}_m}{\hat{\beta}_m} \right] + b \left[\frac{1}{K} \sum_{k=1}^K \frac{E_k(\underline{\delta}) - \hat{E}_k}{\hat{E}_k} \right] \quad (2.3)$$

where a and b are user-defined weights, $\hat{\beta}_m = [\hat{\beta}_m(t); t = 1, \dots, T]$, $m = 1, \dots, M$, are the desired brightness values, and $\hat{E}_k = [\hat{E}_k(t); t = 1, \dots, T]$, $k = 1, \dots, k$ the target energy consumptions. The minimization $\min_{\underline{\delta}} [\Omega(\underline{\delta})]$ has been performed applying the particle swarm evolutionary optimization (PSO) according to the guidelines described in Sub-Section 3.2.2 [27]. [20]

2.2.2.4 Experimental Validation

The proposed system has been installed in two different test sites, which present different geographical and topological characteristics. In particular, the first site is located in the historic center of Trento [Fig. 2.10(a)], the second one in a suburban area on the hills near the city [Fig. 2.10(b)]. A total number of $K = 737$ lamps are individually controlled through a network of $N = 11$ gateways installed in the transformer stations. The details of the network clusters are reported in Tab. 2.1. Before the installation of the monitoring system, a preinstallation measurement campaign has been performed on a selected set of streetlight lines in order to estimate the power consumption of the existing infrastructure in the standard operative configuration.

Test Site	Gateway Index, N	Position	Controlled Lamps, I_n
1	1	Piazza Dante	108
1	2	Piazza Lodron	52
1	3	Via Belenzani	92
1	4	Via S. Giovanni Bosco	24
1	5	Via S. Marco	68
1	6	Via S. Pietro	120
1	7	Vicolo Capitolo	125
1	8	Vicolo Terlago	51
2	9	Via Bellavista	50
2	10	Via del Forte 18	17
2	11	Via del Forte 42	30
Total			737

Table 2.1: Number of Monitored Lamps.

Toward this end, dedicated power meters have been installed in the transformer stations to collect the aggregate power consumptions of the connected electric lines. For comparative purposes, those measurements have been used as reference values to estimate the consumption of the preinstallation configuration assuming the same working schedule determined by the smart monitoring system.

Toward this end, the following active equivalent energy has been estimated

$$\tilde{E} = \left(\tilde{p}^{(day)} \times h^{(day)} \right) + \left(\tilde{p}^{(night)} \times h^{(night)} \right) \quad (2.4)$$

where $\tilde{p}^{(day)}$ is the active equivalent power measured during the daytime slot $h^{(day)}$, while $\tilde{p}^{(night)}$ the one measured during the night hours $h^{(night)}$.

The active powers have been computed as follows starting from the differential energy values

$$\tilde{p}^{(day)} = \frac{\tilde{E}_{end}^{(day)} - \tilde{E}_{start}^{(day)}}{h^{(day)}} \quad (2.5)$$

$$\tilde{p}^{(night)} = \frac{\tilde{E}_{end}^{(night)} - \tilde{E}_{start}^{(night)}}{h^{(night)}} \quad (2.6)$$

where \tilde{E}_{start} and \tilde{E}_{end} are the cumulative energy measured at the beginning and the end of the considered time slot, respectively. A representative comparison between two daily power consumption profiles obtained pre and post installation of the system is shown in Fig. 2.11. The reported values refer to an electric line composed by $I_8 = 51$ streetlight lamps.

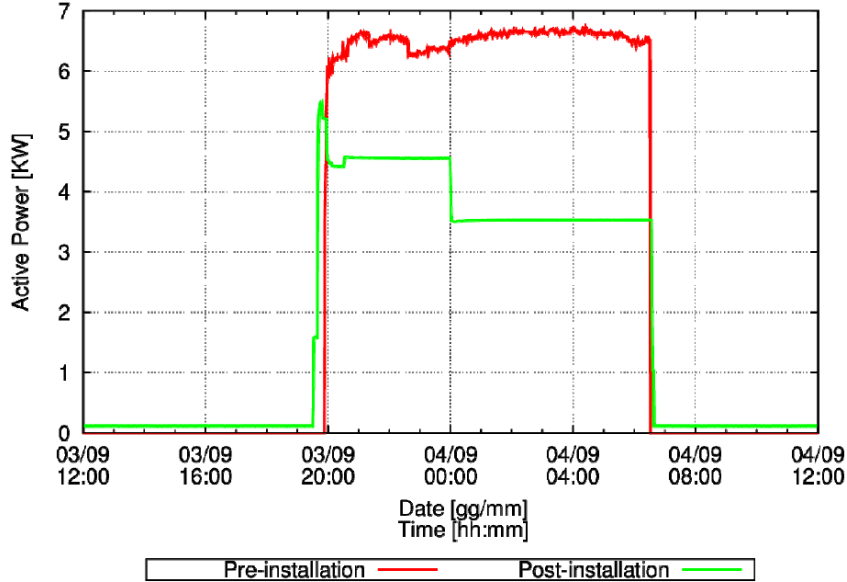


Figure 2.11: Comparison of power consumption profiles *pre* and *post* installation.

As it can be noticed, in the pre-installation configuration the lamps were activated according to a predefined time slot without time-varying dimming profiles. On the contrary, a lower and time-varying power profile has been measured when adaptive dimming rules are applied to the monitored lamps. Such a total profile is the aggregation of the different consumptions of each lamp, which are shown in Fig. 2.12.

The consumptions of the considered lamps differ one from the others because different dimming rules have been configured according to the changing environmental brightness at the street level. The adopted dimming profiles shown in Fig. 2.13 have been calibrated taking in consideration the properties of the lamps as well as the environmental light measured by the lux meters and according to the results of the minimization in (2.3).

The preliminary optimizations have been performed setting the user-defined weights $a = 0.5$ and $b = 0.5$. An example of the lux measurements used for dimming calibration is reported in Fig. 2.14.

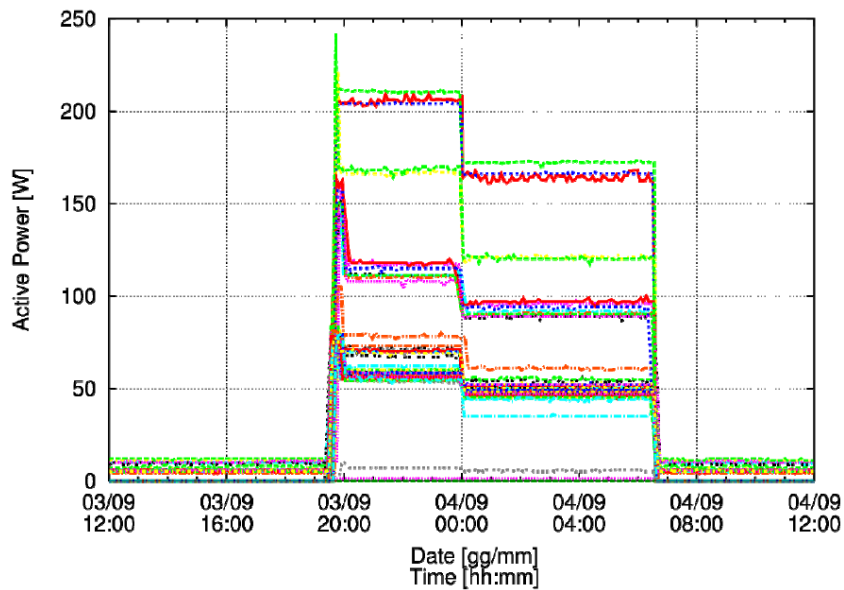


Figure 2.12: Power consumption profiles of the the $I_8 = 51$ controlled nodes.

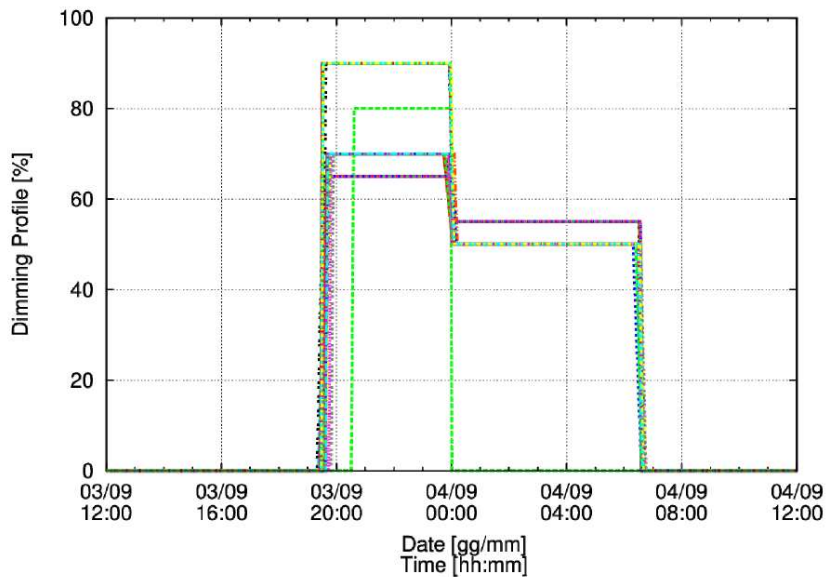


Figure 2.13: Dimming profiles of the the $I_8 = 51$ controlled nodes.

2.2. SYSTEM PROTOTYPES

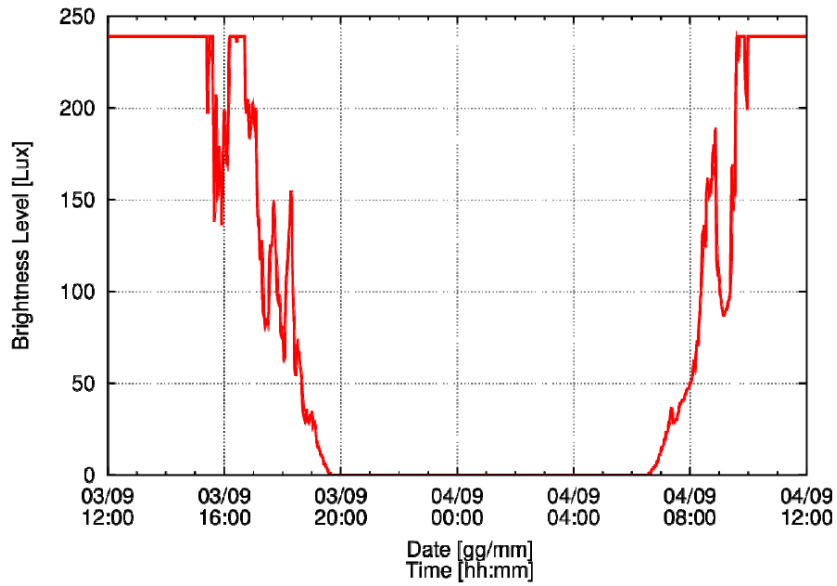


Figure 2.14: Brightness level measured by the lux meter.

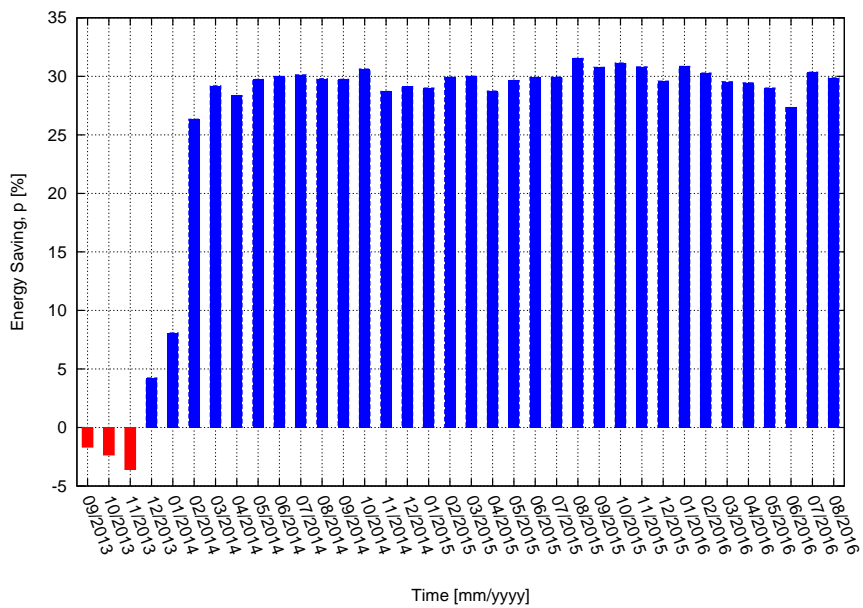


Figure 2.15: Energy saving during the experimental campaign.

The total energy saving has been computed as the normalized difference between the energy consumption *pre* and *post* installation of the monitoring system

$$\delta = \frac{\tilde{E} - E}{\tilde{E}} \times 100 \quad (2.7)$$

where E is the total energy consumption measured by the smart meters integrated in the wireless nodes.

The summary of such percentage saving is reported in Fig. 2.15 for about three-year measurement campaign. The results point out lower savings in the initial months of the monitoring caused by the setup of the devices and the calibration of the system parameters. The following months show a nearly constant energy saving of 30%. [20]

Chapter 3

Distributed Monitoring for Energy Consumption Optimization

The home technology is moving quickly from the programmable thermostat to an era where all home systems will be integrated into a centralized control one, accessible from different entry points such as telephones, computer screens, touch pads, and other wireless mobile devices, like smartphones and tablets. The result is a highly personalized home environment, that reacts to individual needs and wants, and anticipates also changes. This perspective is a clear consequence of the dramatic impact that pervasive technologies have had on society.

In this a framework, a widely diffused viewpoint on the smart home and its implementation, in particular the home automation, is related to the following idea of comfort that can be explained as follows: “Morning brings a graduated alarm that plays some of your favorite music. The volume builds slowly and the bedroom curtains gently part until you react and tell the alarm. Meanwhile, the bathroom floors are already warming in anticipation of your arrival, and the coffee-maker starts brewing up” [28]. The problem complexity, the competition between vendors, the multiple incompatible standards, and the high expenses, together with this idea have limited the penetration of home automation to home. Only a little part of users is disposed today to spend money for those luxury and expensive facilities, because other needs are considered more essential with respect to this strictly comfort-based functionalities. For this reason, much of the potential that would technically be available is still confined to research projects, test beds, or industrial experiments, as shown by the rich state-of-the-art produced in the last years [29]-[33]. Consequently, the researchers are now paying close attention to test and deploy technologies in real environments and for long-term periods by reducing the complexity of this system and implementing solutions providing more evident and tangible advantages to the end users.

Among smart home functionalities, a specific case study of the proposed wireless system is the *Energy Consumption Optimization*. These smart home applications received high emphasis because they have a direct impact on money

saving for both public services and private users.

With the growth of the smart grid research area, concerned with the intelligent control of electricity usage, the smart home plays a key role in the interaction between the grid and the consumers [30]. The end-users' perspective of reducing the costs of in-home power consumptions and the government decisions for optimizing the resources brought to an increasing deployment of the power management systems in private homes all over the world. Many solutions have been proposed for integrating smart meter devices capable of communicating at the same time with both the energy distributors and the household [39], [35]. Toward this end, can be established two main guidelines. The first direction is to collect energy information through the standard utility meter that gives aggregate information about the home consumption [36]. The second direction is to monitor individual appliances of interest by means of in-home distributed smart meters and communicating the recorded data to a central data processing unit [37]. This second solution is sometimes costly and complex to implement because of the need of infrastructure [35]. However, many disadvantages related to costs, wiring, and complexity are going to be overcome thanks to the diffusion of wireless architectures [33], [38]-[45]. [60]

3.1 Distributed Monitoring for Energy Consumption Optimization in Smart Building

In the recent years, the fast growing of the energy market and the need of a more intelligent management of the resources stimulated more and more interactions between the utility companies and their customers, with the aim of optimizing the grid management as well as the energy consumptions and costs. Programs and rules have been developed for the efficient management of the user demands, to reduce waste by encouraging energy-aware consumption patterns, and to obtain more energy efficient buildings [59], [60]. The fundamental requirement of such scenario is the precise knowledge of when and how energy is used by end-users. Many technological solutions exist for the measurement of residential power consumption, usually monitored by utilities at the home level. Improved savings would be possible with direct control of single loads and appliances. To this end, low-cost and noninvasive approaches are required to make such solution feasible and accepted by users. [57]

From the technological perspective, the main challenges are related to the non-scalable integration of heterogeneous technologies that often cannot communicate together, require hard wiring, are ad hoc designed, and cannot be evolved, updated, or easily replaced. The shortage of a common and flexible infrastructure that host heterogeneous functionalities according to the user needs often comes out, and it represents a key challenge that have to be considered in the development of smart home concepts.

Because of these problems, is considered to be inevitable taking advantages of wireless networks as a means for remote monitoring and commanding. Different wireless technologies have been reviewed [33], [46] and applied to smart metering [38], [40], [42], [45], [47], underlining advantages and limitations of current solutions. As a key requirement, the wireless backbone components must be easy to deploy and maintain, inexpensive enough, and making them widely acceptable to end users. Furthermore, it has to be noticed that the the wireless sensor network technology is the most diffused wireless architecture [6, 3, 50]. They have become more and more important because of their ability to manage and monitor information in various intelligent services. The adoption of WSNs in many and heterogeneous applicative fields [48]-[50] has been stimulated by their well-known features like low power, scalability, integrability, low-cost, multisensing, and reconfigurability. These advantages have been transferred to a smart home environment to fulfill the vision of ambient intelligence through an responsive, interconnected, intelligent, and transparent wireless backbone layer. To exploit the technological advantages of WSNs in managing real-time and contextaware applications without directly capturing privacy sensitive informations is the most important challenge of this work. [60]

Starting from the advanced features provided by a dense wireless network architecture (respect to limitations of standalone devices), also the possibility

to actively interact with the monitored environment and change its state according to the rules of adaptive algorithms can be exploited. This bidirectional interaction between the system and the environment requires, besides the actuator devices (able to influence the conditions of the measured scenario), also a userfriendly interface to keep the user in the loop in a transparent way. [57]

For this reason, the advantages of WSN technology have been fused with those of smart control strategies with the final objectives of:

1. making available the user consumption patterns to the energy providers for better management of power grids and peak loads;
2. supporting the end-users of a smart building in the everyday decisions by suggesting optimal solutions for energy cost reduction through improved awareness and optimal habits.

3.1.1 System Architecture

Different wireless technologies have been incorporated at home due to cost effectiveness, flexibility, interoperability, and the consequent improvements in many smart home applications [33], [51]. The proliferation of well-known wireless standards like ZigBee, WiFi, Bluetooth and Z-Wave can be considered at the same time an advantage from a technological point of view, but a commercial drawback [42]. Many investors consider that today's situation is still unstable and they wait to understand which emerging standard will consolidate. For this reason, many solutions are still under investigation, and many real test beds have been deployed with good outcomes. The large diffusion of smart home systems based on WSN technology [39], [52], [53] confirms the feasibility of this technology designed to merge the computational and physical infrastructures and that allows smooth integration of new services and functionalities. One of the most diffused wireless standard is the IEEE 802.15.4 [54], designed for low-power wireless personal area networks (WPAN) with low data rate up to 250 kb/s. IEEE 802.15.4 has been used as a basis for higher layer protocols such as the well-known ZigBee, developed by the ZigBee Alliance [55], that incorporates predefined networking and routing functionalities for easy network management. ZigBee fits the smart home market thanks to its characteristics, and many compliant devices are already available for sale. Many efforts have been devoted to provide ready-to-use devices that require very simple configurations in order to enable the creation of distributed wireless networks among the home rooms. It has been claimed that, even if in some cases ZigBee underperforms with respect to other communication standard [56], the arising key advantages like low cost, network self-organization, and low power make this communication standard a good solution for smart home services.

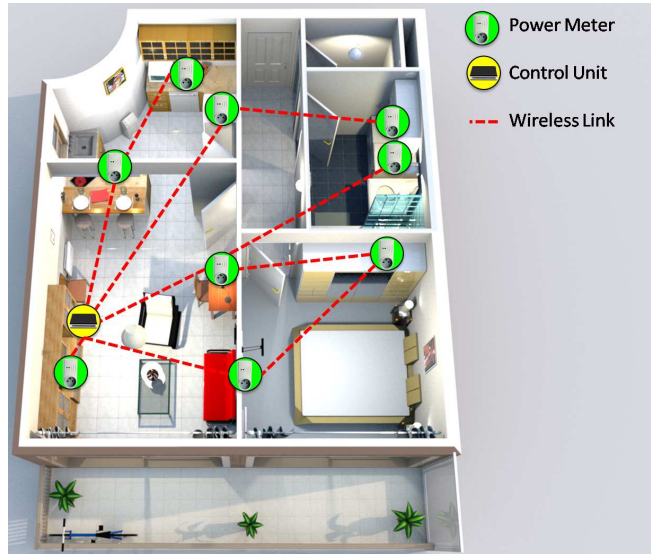


Figure 3.1: Wireless architecture in smart home test site.

By assuming the adoption of ZigBee wireless devices and using the corresponding terminology, our WSN architecture deployed for smart home applications is composed by a set of routers (power meters) plugged in power outlets (ensuring the near absence of battery maintenance), supporting mesh network typology, and associated to a network coordinator that manages the network and collects all the data (Fig. 3.1). The coordinator is interconnected to a control unit like a smart TV, laptop, home gateway, etc., to enable data processing, forwarding, and visualization.

The physical quantities under test, including real-time [W] and cumulative [Wh] power, are acquired by the sensors in a continuous and pervasive way. Such information are locally stored on the node for simple pre-processing and data consistency check, and successively sent throughout the wireless network towards the home gateway control unit.

The communication among the nodes and the gateway are bidirectional to enable both the data acquisition and the appliances control through actuators. The WSN nodes integrate the capability to turn on and off the attached appliances, thus enabling adaptive management of the total load.

3.1.2 Control Strategy

The data acquired during the sensing phase represent the input to the processing step, that implements the proposed Decision Support System (DSS). According to the predefined objectives, this step aims at the real-time evaluation of changes that should be applied to the user load profile.

Different methodological solutions have been explored to manage the optimization of consumptions in presence of multiple and conflicting constraints (e.g., all the users would pay less). Optimization algorithms based on evolutionary strategies [27] usually fit the needs of heterogeneous applications because of their ability in facing with high number of unknowns and multi-minima problems. Genetic algorithms (GA) [27] have been also proposed at the state of the art in the field of sensing and actuation systems. Learning by example (LBE) methodologies [61] also present good matching in the implementation of unsupervised approaches for automatic prediction of system states and estimation of unknown patterns for optimal actuation strategies.

The objective of the optimization is to minimize the total energy cost in the multi-user system. The awareness on cost reduction thanks to a shared pricing mechanism stimulates the users to cooperate. This approach has been formulated through a Game Theoretic (GT) analysis [62]. With an appropriate pricing scheme, the Nash equilibrium of the energy consumption game among the participating users (who share the same energy source) is the optimal solution. Once the problem has been optimized all the users pay less (i.e., when the set of actions for which any user has an unilateral incentive to change actions is found). The cost function to be minimized is mainly regulated by the energy cost, and the unknowns of the optimization problem are the load profiles of all the users, to be adapted in order to reduce as much as possible the peak loads (it is assumed that energy peaks correspond to higher energy costs). [57]

In the following will be defined the main building blocks of the proposed GT-based approach. [58]

3.1.2.1 The Players

The P end users are the players of the game and A_p appliances are controlled by each p th user. A daily energy profile is associated to each player

$$E_p(t) = \sum_{a_p=1}^{A_p} C_{a_p}^p(t) \quad p = 1, \dots, P \quad (3.1)$$

t is the time instant, while $C_{a_p}^p(t)$ ($a_p = 1, \dots, A_p$) being the consumption of the a th home appliance of the p th user/player. The time-varying profiles of the consumptions at every a th appliance $\{C_{a_p}^p(t); a_p = 1, \dots, A_p\}$ are measured in real time by a set of wireless power meters, wirelessly interconnected in a multihop fashion to a gateway node dedicated to data collection and storage. The WSN-based architecture is devoted to both monitor the appliance's loads ("sensing" phase) and control/change their on/off status during the consequent "actuation" phase [2]. The total energy profile of this multiplayer scenario is measured at the building level and it is defined as the sum of the energy consumption of all P lodger of the analyzed building.

$$\Omega(t) = \sum_{p=1}^P E_p(t) \quad (3.2)$$

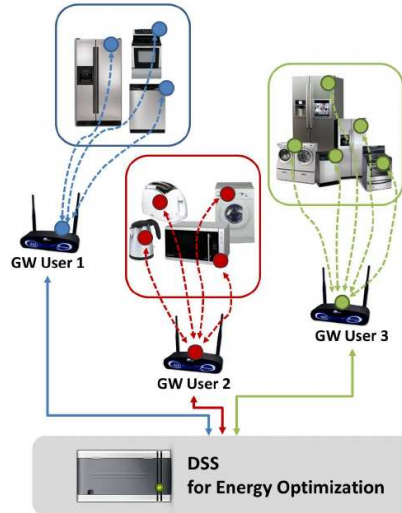


Figure 3.2: System architecture for energy monitoring and optimization.

3.1.2.2 The Game Actions

Every player/user can control the so-called shiftable loads (i.e., those appliances whose usage can be shifted in time according to the user's preference), and can't control the not shiftable loads (i.e., refrigerator, freezer, etc.). Mathematically, the control of shiftable loads is represented by a binary variable $b_{a_p}^p$

$$\begin{aligned} b_{a_p}^p &= 1 && \text{Appliance On} \\ b_{a_p}^p &= 0 && \text{Appliance Off} \end{aligned} \quad (3.3)$$

with $(a_p = 1, \dots, A_p; p = 1, \dots, P)$. Let us suppose that:

1. all the A_p appliances of each p th user are shiftable loads that can be turned on/off from the user itself;
2. all the P users play the "game" with the same rules,;
3. each p th user can implement a personalized strategy according to its own awareness.

3.1.2.3 The Reward

From the user's perspective, the goal of the game is the reduction of the energy bill and the reward of each user is the saving of money that will be reached

through energy cost reduction. The way of limiting the use of the appliances is a trivial option and it is not considered as a viable solution. The energy cost depends from the total energy profile in a nonlinear fashion, we can refer to the following quadratic relation for the energy cost [63]

$$C(\Omega, t) = \alpha(t)\Omega(t)^2 \quad (3.4)$$

where $\alpha(t)$ is a calibration coefficient set by the utility to determine its own cost tariff. In such a model, when there are peaks of energy consumptions (i.e., high values of the total energy profile) the energy cost rapidly increases. To maximize the player's reward we have to minimize the energy cost

$$C_{opt} = \min_{\bar{b}(t)} C(\Omega, t) = \min_{\bar{b}(t)} \left[\alpha(t) \sum_{p=1}^P E_p(t) \right]^2 \quad (3.5)$$

where $\bar{b}(t) = \{\bar{b}_p(t); p = 1, \dots, P\}$, being $\bar{b}_p(t) = \{b_{a_p}^p; a_p = 1, \dots, A_p\}$. From the GT viewpoint, the solution of (3.5) is the so-called Nash equilibrium [62] that holds true *“when no user would benefit by deviating from the evaluated schedule”*. Because of the convexity of the optimization problem at hand (3.5), a convex programming (CP) technique [64] can be applied. More specifically, to make each user independent and to avoid sharing personal behaviors, the optimal solution of (3.5) from a GT viewpoint is reached by solving with CP the following P independent and local optimization problems.

$$\bar{b}_p^{opt}(t) = \operatorname{argmin}_{\bar{b}_p(t)} \left\{ \alpha(t) \left[E_p(t) + \sum_{g=1, g \neq p}^P E_g(t) \right]^2 \right\} \quad p = 1, \dots, P \quad (3.6)$$

When the Nash equilibrium is reached, the peak-to-average ratio (PAR) [59]

$$PAR(t) = \frac{\max_{t \in \{T_m \div T_M\}} [\Omega(t)]}{1/(T_M - T_m) \int_{T_m}^{T_M} \Omega(t) dt} \quad (3.7)$$

is minimized, as well, with $\{T_m \div T_M\}$ the considered time window. The reduction of the PAR and its time stability are a quality indicator of the optimized solution.

3.1.3 Numerical and Experimental Results

The approach proposed in this Section has been validated running several numerical simulations to evaluate the efficacy of the GT-based approach, while a preliminary experimental test has been implemented to give some insights on the real use of the WSN-based monitoring system.

3.1.3.1 Numerical Validation

This first numerical simulation is a representative example of the performance of the system. In this case we consider $P = 8$ players each controlling $A_p = 10$

($p = 1, \dots, P$) loads with different nominal power consumptions and usage time windows. For example, the appliance $a = 3$ of the user $p = 2$ models a dryer with a time-window use in the range $t \in \{5 : 00PM \div 8 : 00PM\}$ and a consumption of $C_3^2(t) = 1.2$ KW. As for the energy cost model, the calibration coefficient in (3.4) has been defined as follows

$$\alpha(t) = \begin{cases} 0.2 \text{ cent} & t \in \{10 : 00PM \div 7 : 00AM\} & (\text{night}) \\ 0.3 \text{ cent} & t \in \{7 : 00AM \div 10 : 00PM\} & (\text{day}) \end{cases} \quad (3.8)$$

The GT-based approach has been used and the optimized appliance schedules have been evaluated by executing the P CP optimizations of (3.6) in a random order to reach an unbiased solution. By applying the GT-optimized appliance scheduling the reached total energy profile $\Omega(t)$ is represented in Fig. 3.4, while the original schedule of the loads and the optimized one of the first user ($p = 1$) are shown in Fig. 3.3). The energy peak reduction improvement with respect to the nonoptimized case turns out to be equal a decrease of the PAR of 43.01% from $PAR = 2.26$ down to $PAR = 1.29$. [58]

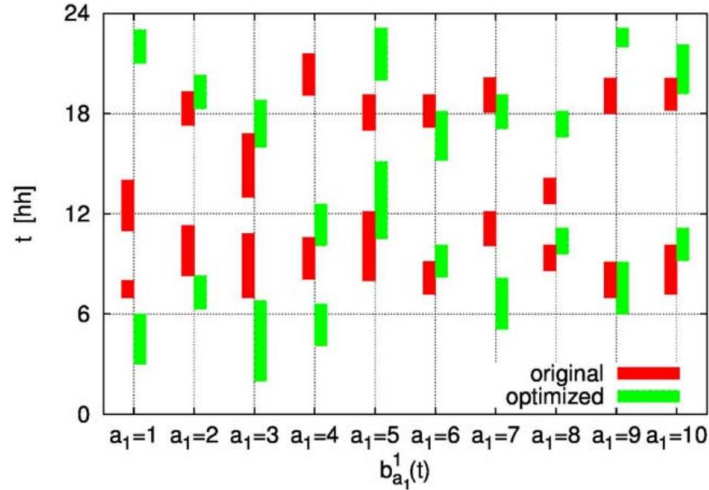


Figure 3.3: Player 1 - appliances schedule before and after optimization.

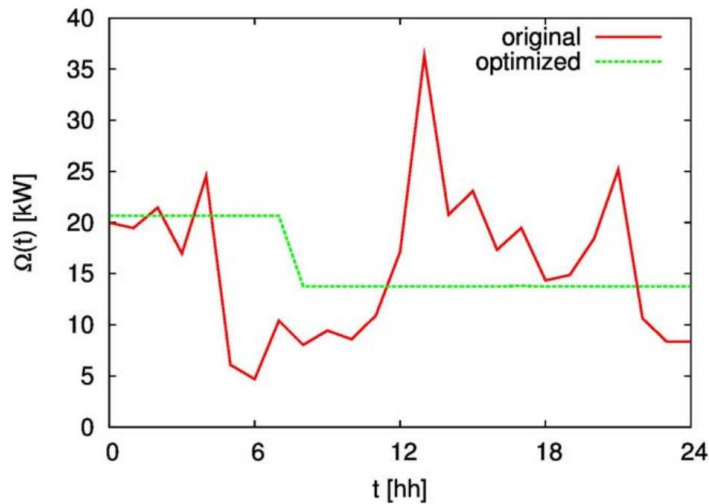


Figure 3.4: Original versus optimized energy profiles.

To give an extended evaluation of the algorithm, multiple simulations have been run to test it in different configurations. In the following are reported the two additional test cases:

1. Varying the number of users P that play the game;
2. Changing the appliance's time-slot configuration.

Varying the Number of Users P In this test case the number of the users P that play the game has been varied from 2 to 10. In Fig. 3.5 are reported the results for $P = 2$ [Fig. 3.5(a)], $P = 4$ [Fig. 3.5(b)], $P = 6$ [Fig. 3.5(c)], $P = 8$ [Fig. 3.5(d)] and $P = 10$ [Fig. 3.5(e)].

From these graphs can be made these three main considerations:

1. Increasing the number of users P , the amount of total energy profile increases (more users mean more appliances);
2. The algorithm is able to optimize the power consumption for each number of users P , minimizing the PAR of total energy profile $\Omega(t)$;
3. The PAR at the end of each simulation is almost the same (Tab. 3.1).

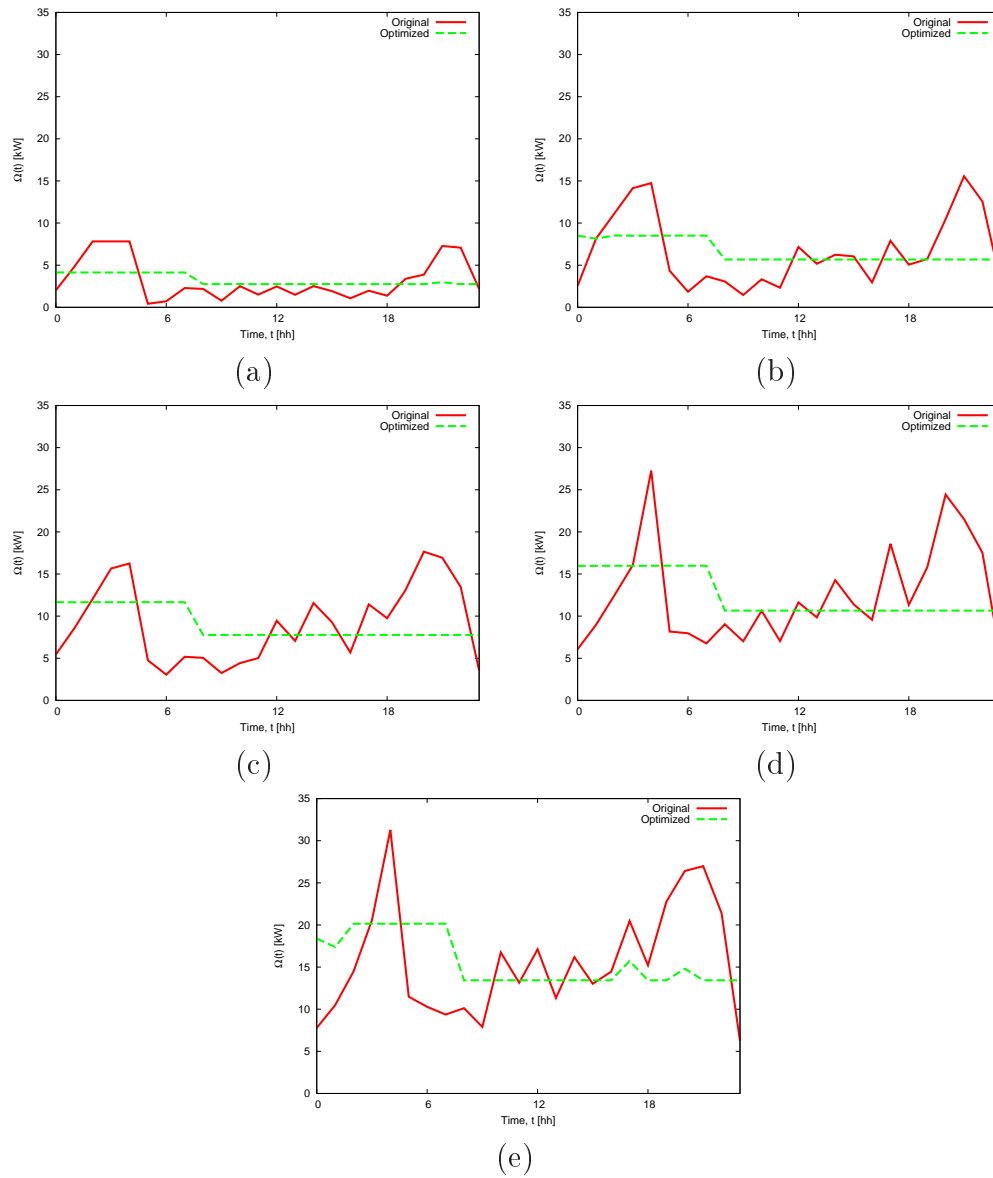


Figure 3.5: Performances of the GT-based approach varying the number of users P : (a) $P = 2$, (b) $P = 4$, (c) $P = 6$, (d) $P = 8$ and (e) $P = 10$.

3.1. DISTRIBUTED MONITORING FOR ENERGY CONSUMPTION OPTIMIZATION IN SMART BUILDING

Number of User P	Optimized PAR
2	1.282
4	1.289
6	1.286
8	1.286
10	1.288

Table 3.1: PAR values after the CP Optimizations.

Changing the Appliance’s Time-Slot Configuration In this test case an option has been integrate inside the algorithm: each user can limit the duration of the time slots in which the algorithm can move the scheduling of each appliance. Three main contitions have been defined:

1. Ideal: the time slot are not present and the algorithm can place the appliance scheduling at every hour of the day;
2. Real: each user can choose, for each shiftable appliance, a time slot with a duration of about 8/9 hours, in which its usage can be scheduled by the algorithm;
3. Complex: each user can choose, for each shiftable appliance, a time slot with a duration of about 5/6 hours, in which its usage can be scheduled by the algorithm;

In Tab. 3.2, Tab. 3.3 and Tab. 3.4 are respectively reported the experimental time slots set for each condition (the appliances followed by $N.S.$ are not shiftable).

CHAPTER 3. DISTRIBUTED MONITORING FOR ENERGY
CONSUMPTION OPTIMIZATION

<i>User p:</i>	#1	#2	#3	#4	#5	#6	#7	#8	#9	#10
<i>Appliances a_p:</i>										
Phev	0-23	0-23	0-23	0-23			0-23	0-23	0-23	0-23
Food Cutter			0-23	0-23						
Dryer			0-23	0-23	0-23			0-23		0-23
Vacuum Cleaner	0-23	0-23	0-23	0-23	0-23	0-23		0-23		
Dehumidifier					0-23	0-23	0-23		0-23	0-23
Electric Iron		0-23	0-23	0-23	0-23	0-23	0-23		0-23	0-23
Oven	0-23	0-23	0-23	0-23	0-23	0-23	0-23	0-23	0-23	0-23
Dishwasher	0-23	0-23	0-23	0-23	0-23	0-23	0-23	0-23	0-23	0-23
Washing Machine	0-23	0-23	0-23	0-23	0-23	0-23	0-23	0-23	0-23	0-23
Pasta Maker		0-23	0-23		0-23	0-23	0-23			0-23
Microwave		0-23	0-23		0-23		0-23	0-23		0-23
Hair Dryer	0-23	0-23	0-23		0-23			0-23	0-23	0-23
Sauna	0-23				0-23		0-23			0-23
Alarm Clock (<i>N.S.</i>)	0-23	0-23	0-23	0-23		0-23		0-23	0-23	
Stereo (<i>N.S.</i>)	0-23			0-23		0-23		0-23	0-23	
Air-Conditioning (<i>N.S.</i>)	0-23	0-23				0-23	0-23		0-23	
Light (<i>N.S.</i>)	0-23	0-23	0-23	0-23	0-23	0-23	0-23	0-23	0-23	0-23
Freezer (<i>N.S.</i>)	0-23	0-23		0-23	0-23	0-23	0-23	0-23	0-23	
Refrigerator (<i>N.S.</i>)	0-23	0-23	0-23	0-23	0-23	0-23	0-23	0-23	0-23	0-23
Computer (<i>N.S.</i>)	0-23			0-23		0-23	0-23	0-23	0-23	0-23
Television (<i>N.S.</i>)	0-23	0-23	0-23	0-23	0-23	0-23	0-23	0-23	0-23	0-23

Table 3.2: Time-Slot for each user in “ideal” condition.

3.1. DISTRIBUTED MONITORING FOR ENERGY CONSUMPTION OPTIMIZATION IN SMART BUILDING

<i>Appliances a_p:</i>	<i>User p:</i>									
	#1	#2	#3	#4	#5	#6	#7	#8	#9	#10
Phev	0-8	0-9	2-10	0-8			0-9	0-10	1-10	0-8
Food Cutter			11-20	12-20						
Dryer			0-8	14-22	15-23			14-23		0-9
Vacuum Cleaner	10-19	10-19	6-15	10-20	9-18	10-18		7-16		
Dehumidifier					9-18	15-23	15-23		10-20	14-22
Electric Iron		14-22	13-22	6-15	9-18	14-23	13-23		10-19	9-18
Oven	11-20	12-20	11-19	12-21	11-19	11-19	12-20	11-21	11-19	12-20
Dishwasher	13-22	12-21	14-23	14-22	13-21	15-23	13-22	13-21	12-22	13-23
Washing Machine	0-10	15-23	0-9	15-23	0-9	0-8	0-9	10-20	11-19	15-23
Pasta Maker		15-23	6-14		7-16	11-19	14-22			7-16
Microwave		12-20	11-19		11-20		12-20	11-20		12-20
Hair Dryer	15-23	15-23	6-14		8-16			15-23	6-14	15-23
Sauna	15-23				14-22		14-23			14-23
Alarm Clock (<i>N.S.</i>)	0-23	0-23	0-23	0-23		0-23		0-23	0-23	
Stereo (<i>N.S.</i>)	0-23			0-23		0-23		0-23	0-23	
Air-Conditioning (<i>N.S.</i>)	0-23	0-23				0-23	0-23		0-23	
Light (<i>N.S.</i>)	0-23	0-23	0-23	0-23	0-23	0-23	0-23	0-23	0-23	0-23
Freezer (<i>N.S.</i>)	0-23	0-23		0-23	0-23	0-23	0-23	0-23	0-23	
Refrigerator (<i>N.S.</i>)	0-23	0-23	0-23	0-23	0-23	0-23	0-23	0-23	0-23	0-23
Computer (<i>N.S.</i>)	0-23			0-23		0-23	0-23	0-23	0-23	0-23
Television (<i>N.S.</i>)	0-23	0-23	0-23	0-23	0-23	0-23	0-23	0-23	0-23	0-23

Table 3.3: Time-Slot for each user in “real” condition.

CHAPTER 3. DISTRIBUTED MONITORING FOR ENERGY
CONSUMPTION OPTIMIZATION

<i>User p:</i>	#1	#2	#3	#4	#5	#6	#7	#8	#9	#10
<i>Appliances a_p:</i>										
Phev	0-6	6-12	1-7	2-8			0-6	5-12	1-7	1-8
Food Cutter			11-16	12-17						
Dryer			0-7	17-23	0-6			17-22		0-6
Vacuum Cleaner	6-11	6-12	7-13	7-13	6-11	10-16		7-14		
Dehumidifier					10-17	11-18	9-16		15-22	11-18
Electric Iron		15-20	14-20	14-19	15-20	14-20	14-20		16-21	9-15
Oven	17-23	11-17	18-23	11-17	11-17	17-23	12-19	18-23	17-22	11-18
Dishwasher	18-23	12-18	18-23	13-20	12-19	18-23	13-20	18-23	13-20	12-17
Washing Machine	0-7	17-22	0-6	0-6	0-6	17-22	0-7	0-6	2-8	17-23
Pasta Maker		17-22	7-13		17-22	17-22	7-13			7-13
Microwave		10-17	18-23		12-18		10-17	17-22		11-16
Hair Dryer	7-12	6-11	6-11		8-13			6-12	7-12	6-11
Sauna	18-23				17-23		16-23			17-22
Alarm Clock (<i>N.S.</i>)	0-23	0-23	0-23	0-23		0-23		0-23	0-23	
Stereo (<i>N.S.</i>)	0-23			0-23		0-23		0-23	0-23	
Air-Conditioning (<i>N.S.</i>)	0-23	0-23				0-23	0-23		0-23	
Light (<i>N.S.</i>)	0-23	0-23	0-23	0-23	0-23	0-23	0-23	0-23	0-23	0-23
Freezer (<i>N.S.</i>)	0-23	0-23		0-23	0-23	0-23	0-23	0-23	0-23	
Refrigerator (<i>N.S.</i>)	0-23	0-23	0-23	0-23	0-23	0-23	0-23	0-23	0-23	0-23
Computer (<i>N.S.</i>)	0-23			0-23		0-23	0-23	0-23	0-23	0-23
Television (<i>N.S.</i>)	0-23	0-23	0-23	0-23	0-23	0-23	0-23	0-23	0-23	0-23

Table 3.4: Time-Slot for each user in “complex” condition.

In Fig. 3.6 are reported the results of the simulations ran in this test case. In the ideal condition the CP algorithm is able to optimize the energy consumptions as in the previous test cases while, in real and complex condition, the algorithm optimizes the energy profiles, but reaches higher *PAR* values as reported in Tab. 3.5. In these cases the algorithm reaches a sub-optimal solution. It is not able to reach the optimal *PAR* value because it has to match the constraint set by each user in a more realistic scenario.

3.1. DISTRIBUTED MONITORING FOR ENERGY CONSUMPTION OPTIMIZATION IN SMART BUILDING

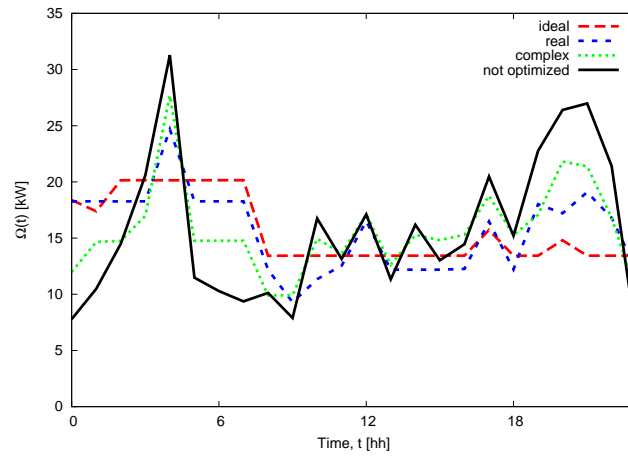


Figure 3.6: Performances of the GT-based approach varying the time slot conditions.

Contition	PAR
Not Optimized	2.001
Ideal	1.288
Real	1.578
Complex	1.770

Table 3.5: PAR values after the CP Optimizations varying the time slot conditions.

3.1.3.2 Experimental Results

The proposed system has been experimentally tested and a preliminary set of results have been selected to assess the potentialities and limitations of both the monitoring WSN based architecture and the DSS for energy optimization and cost reduction in smart buildings.

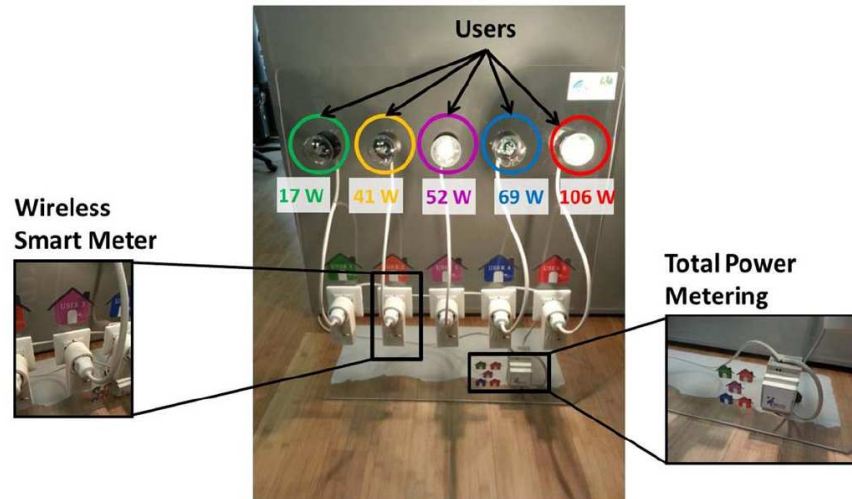


Figure 3.7: Experimental setup for wireless power metering and control.

As for the experimental validation, a demonstrative prototype has been built (Fig. 3.7) with WSN nodes equipped with Zigbee compliant wireless power meters able to:

1. acquire in real-time the power consumption;
2. switch (on/off) the interconnected loads;
3. dimmer the output power.

A network of $P = 5$ WSN nodes have been connected to a set of lamps, which represent the user's loads, and the changes of the players' power consumption have been simulated by dimming the lamps. A centralized power meter has been added to measure the total power (modeling the power consumption of whole building). All the powers measured by this devices have been transmitted to a control unit equipped with a Zigbee coordinator. The control unit has been dedicated to execute and actuate the GT-based scheduling by controlling the wireless power meters, and for easy data visualization and system management. An example of the graphical user interface of the developed web tool is shown

3.1. DISTRIBUTED MONITORING FOR ENERGY CONSUMPTION OPTIMIZATION IN SMART BUILDING

in Fig. 3.8. The output of the DSS that is the optimal suggestion about when and how use the appliances has been made available to the users. The automatic management of the appliances has been also implemented and, if activated by the user, the on/off schedule is automatically applied through the WSN actuators.



Figure 3.8: Graphical interface for data visualization and management.

By considering an analysis of 24-h experimental data, it turns out that the GT-based optimization has been able to reduce the PAR value from 2.08 down to 1.54 (i.e., a decrease of 25.19%) with a corresponding energy cost reduction (deduced from the real tariffs of the utility) from 35.31 \$ e to 32.09 \$ e (i.e., a cost saving of 9.22%).

3.2 Wireless Smart Lighting in Energy-Efficient Museums

In the application field of smart museums, a strong attention has been given to the lighting quality, mainly from the perspective of the visitors and with respect to the artworks' conservation [66]. However, less attention has been given to the energy saving. The management of multiple and competing objectives is not straightforward and requires a suitable strategy to support the decision of the museum energy manager in the control of the lighting systems. In this Section, an evolutionary optimization strategy based on particle swarm optimization (PSO) [27] is proposed to control the light intensity of multiple lamps taking in consideration both the quality of the user experience and the energy saving. The wireless sensor and actuator (WSAN) technology [2] has been exploited to sense the environmental condition and the energy consumption as well as to control the lamp actuators. The proposed system provides an innovative solution to the energy managers for the autonomous light dimming, which satisfies the desired requirements even in complex museum rooms. The system has been deployed and tested in a museum scenario in order to experimentally assess the performance in terms of lighting quality of artworks and energy saving. [65]

3.2.1 Wireless Architecture

In this system N wireless nodes for the acquisition of the light intensity are installed in the points of interests $\underline{r}_n^{(s)}$, $n = 1, \dots, N$, close to the artworks to be properly illuminated (Fig. 3.9). Each node is equipped with environmental sensors including the lux meter for the measurement of the light intensity l_n , $n = 1, \dots, N$. M wireless actuators are integrated in the smart lamps of the lighting system, in positions $\underline{r}_m^{(a)}$, $m = 1, \dots, M$, and are devoted to control the dimming levels d_m , $m = 1, \dots, M$, computed by the centralized actuation strategy. The light intensities determine the power consumptions p_m , $m = 1, \dots, M$ of the museum. The wireless network is managed by a local coordinator, which hosts the proposed smart lighting algorithm.[65]

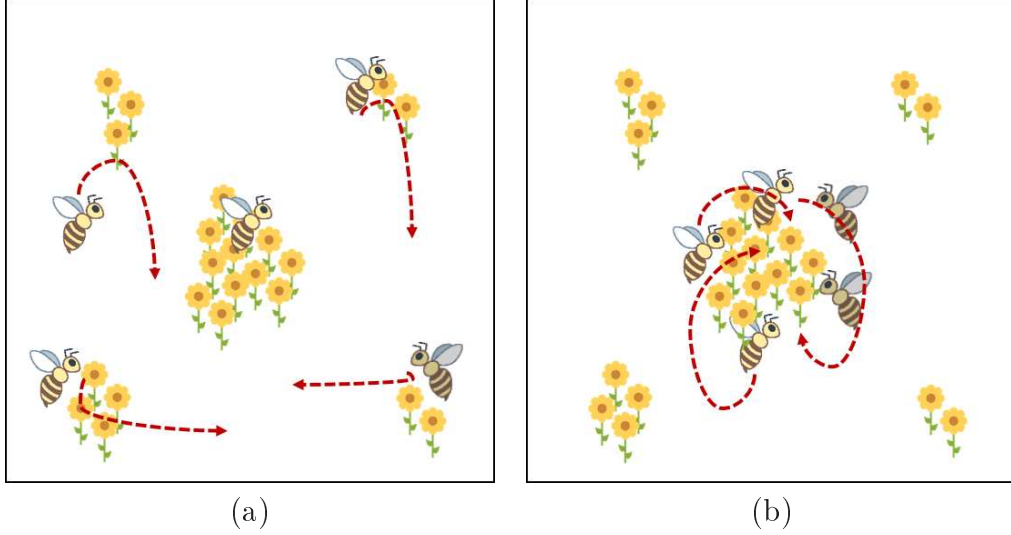


Figure 3.10: Particle Swarm Optimizer: (a) Bees searching a field for the location of the most flowers (b) All the bees swarm around the best location.

3.2.2.1 Mathematical Formulation

In Particle Swarm Optimizer, an agent, $b_k^{(p)}$, called particle is characterized by a position $f_k^{(p)}$ in the solution space and a velocity $v_k^{(p)}$ that models the capability of the p th particle to fly from the current position to another successive position $f_{k+1}^{(p)}$. The whole set of particles $\{b_k^{(p)}, p = 1, \dots, P\}$ constitutes the swarm F_k . In its classical implementation [76], the particle update equations are

$$f_{k+1}^{(p)} = f_k^{(p)} + v_{k+1}^{(p)} \quad (3.9)$$

and

$$v_{n,k+1}^{(p)} = \omega v_{n,k}^{(p)} + C_1 r_1 (p_{n,k}^{(p)} - f_{n,k}^{(p)}) + C_2 r_2 (g_{n,k} - f_{n,k}^{(p)}) \quad (3.10)$$

whose physical interpretation, derived by Newton' laws, has been given in [78]. In (3.10), ω , C_1 and C_2 are control parameters known as inertial weight, cognitive and social acceleration terms, respectively [77]. Moreover, r_1 and r_2 are two random variables having uniform distribution in $[0, 1]$. With reference to a minimization problem, the values $p_k^{(p)} = \arg\{\min_{i=1, \dots, k} [\Phi(f_i^{(p)})]\}$ and $g_k = \arg\{\min_{i=1, \dots, k; p=1, \dots, P} [\Phi(f_i^{(p)})]\}$ are the so-called *personal* and *global* best solutions, namely the best positions found by the p th particle and by the whole swarm until iteration k , respectively.

3.2. WIRELESS SMART LIGHTING IN ENERGY-EFFICIENT MUSEUMS

As far as the iterative optimization is concerned (Fig. 3.11), starting from guess values of $\underline{f}_0^{(p)}$ and $\underline{v}_0^{(p)}$, $p = 1, \dots, P$, the positions and velocities of the particles are updated according to equations (3.9) and (3.10).

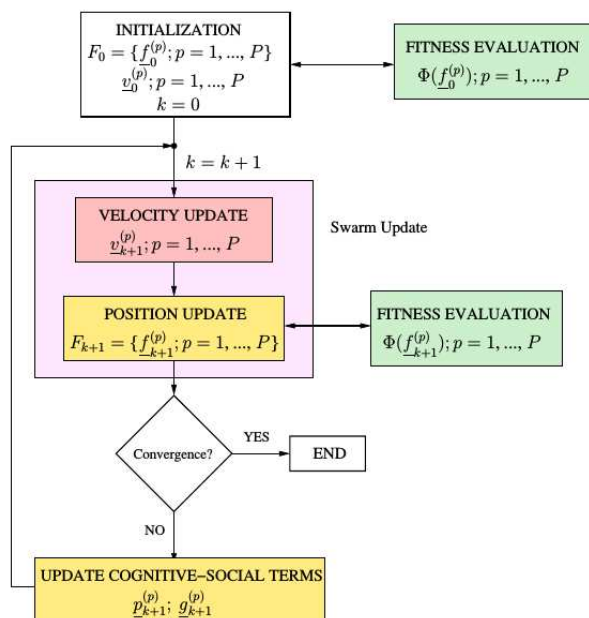


Figure 3.11: Particle swarm optimizer: flowchart.

The main advantages of the PSO if compared to other optimization techniques as the Genetic Algorithms (GAs) or Differential Evolution (DE) can be summarized in the followings:

- the simplicity of the algorithm implementation and the use of a single operator (i.e., the velocity update) instead of three genetic operators (i.e., the crossover, the mutation and the selection);
- the easy manipulation of the calibration parameters [79] (i.e., the swarm size, the inertial weight and the acceleration coefficients) which controls the velocity update operator. Even if the number of control parameters (i.e., the population size, the crossover rate, the mutation rate) is similar, it is certainly easier to set the PSO indices than evaluating the optimal setting among various operators and several options of implementation;
- the ability to prevent the stagnation by controlling the inertial weight and the acceleration coefficients to sample new regions of the solution space. In standard GAs and DE, the stagnation occurs when the trial solutions

assume the same genetic code close to that of the fittest individual. In such a case, the crossover does not contribute to the evolution and only a lucky mutation could locate a new individual in other interesting region of the solution space;

- a smaller number of agents, which turn out in a reduced computational cost of the overall optimization and enable a reasonable compromise between computational burden and efficiency of the iterative process.

Regarding the setting of the parameters, Clerc and Kennedy [68] examined in detail the behavior of the PSO and defined some conditions on the PSO parameters to avoid a divergent search. With reference to a simplified one-dimensional (i.e., $N = 1$) and deterministic ($C_1 r_1 = C_1$ and $C_2 r_2 = C_2$) model, described by the following updating equations

$$\begin{aligned} v_{k+1} &= v_k + \varphi(t - f_k) \\ f_{k+1} &= f_k + v_{k+1} \end{aligned} \tag{3.11}$$

where $\varphi = C_1 + C_2$ and $t = \frac{C_1 p + C_2 g}{C_1 + C_2}$ is the index related to both the cognitive and the social term and by supposing the personal best and global best position fixed (i.e., $p_k = p$ and $g_k = g$), it has been shown that when $\varphi \geq 4$, the particles diverge as a function of k , while when $0 < \varphi < 4$ the trajectories oscillate around the position t [71] with cyclic or quasi-cyclic behavior depending on φ . These conclusions have been drawn from the analysis of (3.11) rearranged in the matrix form as follows: $\mathcal{F}_{k+1} = M\mathcal{F}_k$ where $\mathcal{F}_k = [v_k, z_k]^T$, being $z_k = (t - f_k)$, and the dynamic matrix is given by

$$M = \begin{bmatrix} 1 & \xi \\ -1 & 1 - \xi \end{bmatrix} \tag{3.12}$$

As a matter of fact, it turns out that $\mathcal{F}_k = M^k \mathcal{F}_0$, \mathcal{F}_0 being the initialization vector. A sufficient condition to reach an equilibrium point at the convergence (i.e., t) is that the amplitudes of the two eigenvalues of M are lower than unity [75]. However, a random choice of φ causes the uncontrolled increasing of the velocity term v_{k+1} [77].

Further developing the approach based on the generalized matrix, it has been proved that the following constriction system

$$\begin{aligned} v_{k+1} &= \chi[v_k + C_1 r_1(p - f_k) + C_2 r_2(g - f_k)] \\ f_{k+1} &= f_k + v_{k+1} \end{aligned} \tag{3.13}$$

where $\chi = \frac{2}{|2 - \epsilon - \sqrt{\epsilon^2 - 4\epsilon}|} = 0.7298$ with $\varphi = 2C_1 = 2C_2 = 4.1$ guarantees the stability of the optimization process.

Other variants of the PSO exist and a careful analysis about the convergence taking into account the randomness of the algorithm has been reported in [72].

Concerning the optimal choice of the control coefficients, it is still worthwhile pointing out that since higher values of ω produce relatively straight particle trajectories, resulting in a good global search characteristic, while small values of ω encourage a local searching, some researchers have gained advantage from a decrease [69, 74] or a random variation of ω during the iterations [70]. In regard to the coefficients C_1 and C_2 , they are usually set to 2.0 as recommended by some papers in the PSO literature [76, 77, 73] and found through experimentation in several optimization fields [67]. [27]

3.2.2.2 Custom Fitness Function

The solution to the considered multi-objective problem has been addressed by a customized PSO optimizer through the minimization of the following multi-terms cost function:

$$\Phi(\underline{d}) = \alpha \sum_n \frac{|L_n - l_n(\underline{d}, \varepsilon)|}{L_n} + \beta \sum_m \frac{|P_m - p_m(\underline{d}, \varepsilon)|}{P_m} \quad (3.14)$$

where $\underline{d} = [d_m; m = 1, \dots, M]$ is the set of dimming profiles imposed to the actuators, L_n and P_m are the desired light levels and the desired power consumptions, respectively, ε is the environmental brightness measured outdoor, and α and β are the user-defined weights to balance the impact of the two objectives.

The multi-objective problem has been reformulated in (3.14) as a linear combination of the two conflicting objectives in order to avoid the choice of the best solution among the Pareto optimal ones [27]. The PSO has been adopted since the problem presents many suboptimal solutions, due to the intrinsic complexity of the indoor environment, the overlapping of the light beams, and the time-varying nature of ε , which determines an unpredictable relation between the actuators and the light in the regions of interest. The iterative minimization of (3.14) is aimed at continuously updating \underline{d} in order to reach the desired goals imposed by the museum manager. The targets L_n and P_m , as well as the weights α and β are calibrated according to museum conditions and artworks typologies. [65]

3.2.3 Experimental Validation

The proposed system has been experimentally validated using commercial low-cost devices, both for sensing and actuation to verify the portability of the proposed control strategy on top of existing hardware. The TI SensorTag [Fig. 3.12(a)] based on the ZigBee wireless technology has been selected as a small, low-power, and low-cost multi-sensors platform. The commercial WiFi-based dimmable lamps by Mi-Light [Fig. 3.12(b)] have been adopted to implement the smart actuators.

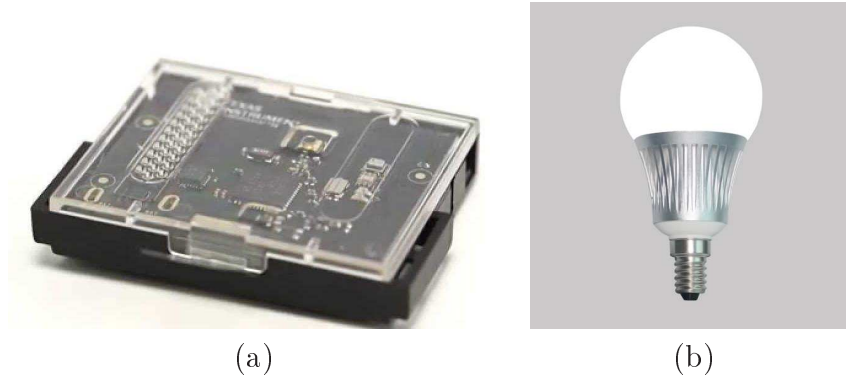


Figure 3.12: Devices used in the experimental validation: (a) TI SensorTag, (b) Mi-Light dimmable lamps.

The multistandard (i.e., both WiFi and ZigBee) coordinator has been implemented with a low-cost Raspberry Pi platform. A smallscale museum area has been equipped with a set of $N = 2$ sensors and $M = 4$ actuators to manage three regions of interest. The protocol for the data acquisition and for the command transmission has been customized to guarantee a system lifetime of at least 6 months, introducing low-power strategies with adaptive duty cycling based on the temporal dynamics of the indoor brightness. Some selected test cases are presented to preliminary show the optimization capabilities. [65]

In the first test-case, the desired power consumptions of 3 W has been set for all the smart lamps and the desired light levels of 500 Lux has been set for all the lux meters. In Fig. 3.13(a), Fig. 3.13(b), Fig. 3.13(c) and Fig. 3.13(d) have been respectively represented: the evolution of the PSO fitness function Φ , the evolution of the light levels L_n , the evolution of the power consumptions P_m , and the evolution of the dimming profiles of the smart actuators d_m .

In the second test-case (Fig. 3.14) has been presented a more general setting of the system, by imposing a custom desired value for every light sensor and smart lamp installed in the system ($TargetL_1 = 400[Lux]$, $TargetL_2 = 500[Lux]$, $TargetP_1 = 2[W]$, $TargetP_2 = 5[W]$, $TargetP_3 = 3[W]$ and $TargetP_4 = 4[W]$).

3.2. WIRELESS SMART LIGHTING IN ENERGY-EFFICIENT MUSEUMS

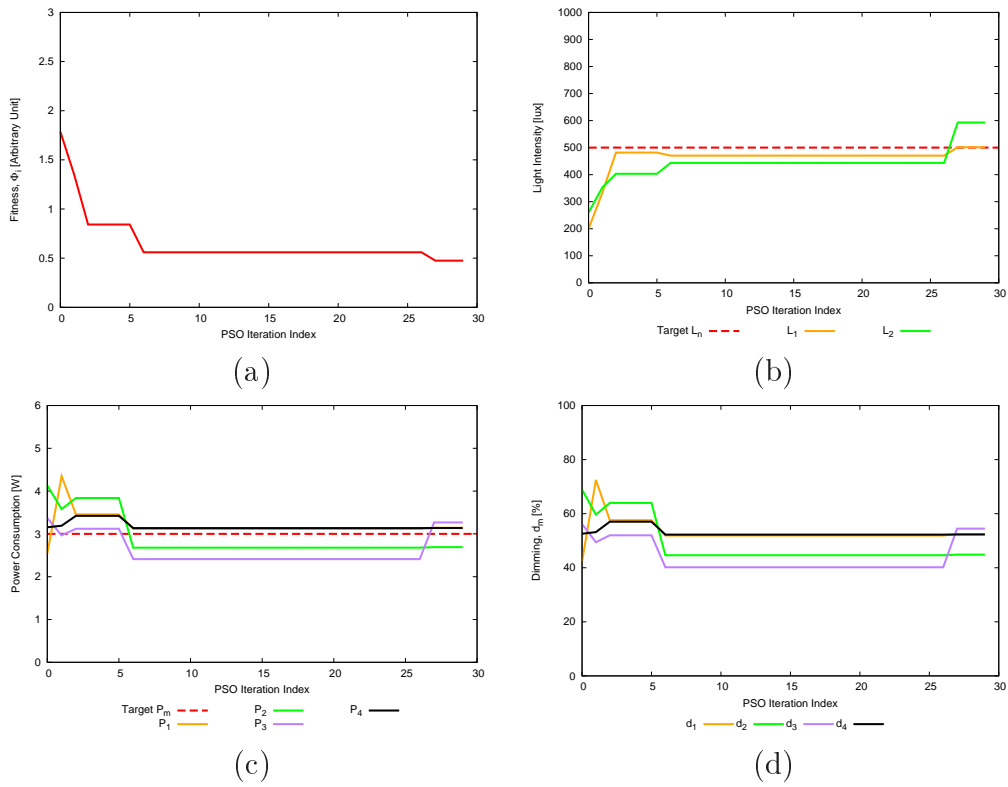


Figure 3.13: Test-case 1: (a) Fitness function evolution, (b) light intensity, (c) power consumption and (d) dimming profiles of the smart actuators in the regions of interest.

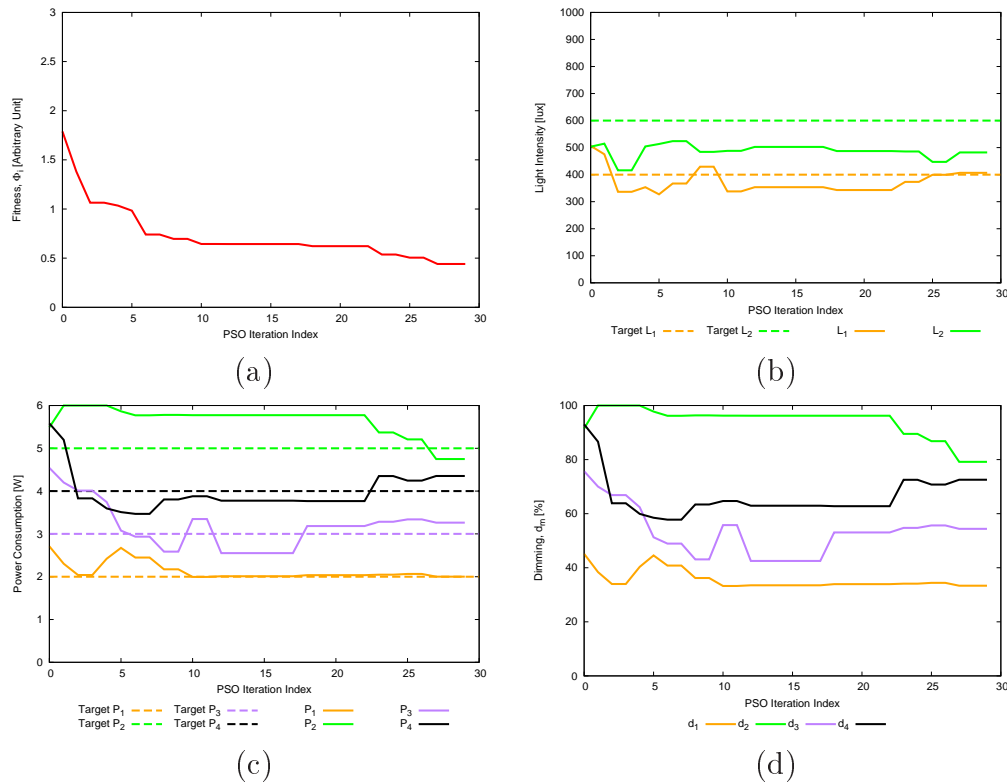
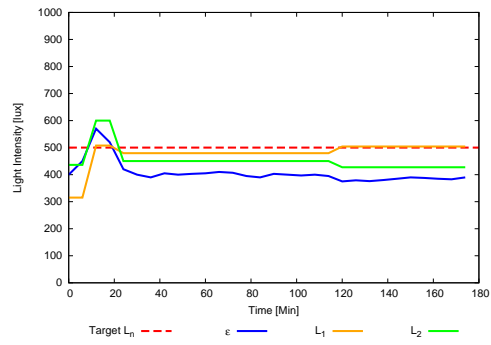


Figure 3.14: Test-case 2: (a) Fitness function evolution, (b) light intensity, (c) power consumption and (d) dimming profiles of the smart actuators in the regions of interest.

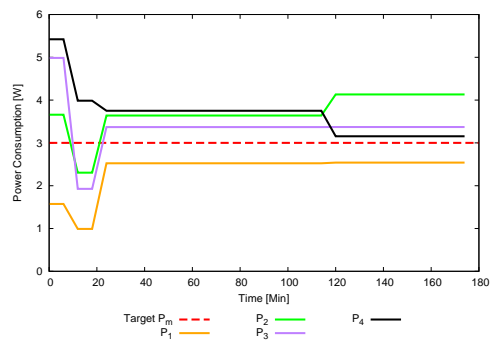
Finally, a third test-case is presented to preliminary show the optimization capabilities with continuous time-varying environmental brightness ε , which has been measured every 6 minutes during this test.

Fig. 3.15 shows the time evolution of the measured lights [Fig. 3.15 (a)], the measured consumptions [Fig. 3.15 (b)] and the computed dimming profiles [Fig. 3.15 (c)] setting uniform cost function weights, $L_n = 500$ [Lux], and $P_m = 60$ [W], which is 40[%] lower than the nominal power of the lamp in order to force the energy saving. The results point out the capability to maintain the variability of light lower than 100 [Lux] in the regions of interest for more than 95 [%] of the 3 hours test duration, even in presence of external environmental changes and with an average energy saving of 37 [%]. The changes of light during the optimization take few milliseconds in order to make the process transparent to the users.

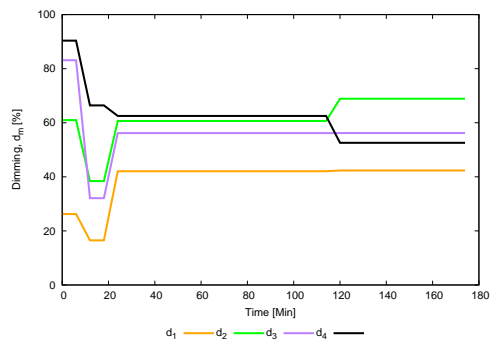
3.2. WIRELESS SMART LIGHTING IN ENERGY-EFFICIENT MUSEUMS



(a)



(b)



(c)

Figure 3.15: Light intensity (a), power consumption in the regions of interest (b), and optimal dimming profiles of the smart actuators (c).

Chapter 4

Opportunistic Occupancy Estimation System for Museum Environments

Museum monitoring systems have been widely adopted for artworks conservation tasks, through the adoption of different monitoring technologies. In this scenario, both wired and wireless sensors have been developed for accurate measurement of physical parameters, that is one of the main concerns in museums. In order to conserve both the artworks and the museum itself (in particular for museum in historic buildings), it is fundamental to continuously measure and control quantities like temperature, humidity, and light. Moreover, in this applicative scenario it is fundamental to minimize the visual impact for esthetical reasons.

The wireless sensor network (WSN) technology has been widely adopted in a variety of application fields [81]-[85] and also in museum scenario it exhibits several suitable features, including: the capability to integrate multiple and heterogeneous sensors on a single small WSN node, the absence of cables or wired invasive infrastructures, the cooperation among the nodes for coverage extension and user interaction, simple and quick system scalability, management of high number of measurement points, high lifetime, and the low cost of the hardware platform. The deployment of a WSN-based monitoring system in museum allows periodical measurements of single artworks (e.g. paintings, sculptures, artifacts), making them an active element of the museum, always connected and remotely controllable [48][49].

The smart cooperation among the WSN nodes allows also to overcome the limitations proper of a single low-power and low-cost device, improving for example the total coverage of the system through the intelligent forwarding of the information throughout the network towards the control unit [86][87][102]. In this Chapter, the architecture, the objectives and the implementation of the proposed WSN-based museum monitoring system are presented. The main challenges related to the deployment in historic buildings as well as the capabilities of such

backbone to adapt according to the specific characteristics and requirements of different museums are described. [80]

Furthermore, in this Chapter, to indirectly estimate the presence of visitors and the museum occupancy will be opportunistically employed the environmental data available for artworks conservation purposes. It is worth pointing out that these information are of paramount importance for a wide set of location-based services, including route planning, flow management, exhibitors positioning, and security issues.

4.1 System Architecture

The architecture of a WSN-based monitoring system can assume different topologies (e.g., star-, tree- and mesh- topology) according to the connection and routing rules established among the network nodes. As an example, in the star-topology one single node is in charge of the network coordination. This solution is very simple but implies a limited wireless coverage (i.e., limited to the single node-node wireless link). A more complex solution is represented by the tree-topology, based on a rigorous hierarchy defining the coordination points along the different tree branches. Each node has to communicate with its nearest parent, namely the network node at the immediately higher level in the hierarchy. As another example, in the mesh-topology each node is connected to the others, thus making the system more robust but contemporarily more complex, given the high number of connections and the consequent consumptions due to more computations and transmissions.

The architecture of the proposed system is based on a hybrid topology composed by two different WSN node types: the *anchor node* and the *sensor node*. The main difference between these two node categories is related to the specific functionalities they are designed for. In particular, a *sensor node* is mainly devoted to sense and acquire environmental parameters through specific sensors directly interconnected within the wireless platform. *Anchor nodes* are mainly devoted to collect the information transmitted by sensor nodes and forward it towards the control unit. The adoption of *anchor nodes* is mainly due to wireless coverage extension and network robustness improvement. Given these tasks, the *anchor nodes* have been designed to be connected also to the power grid, since they have to keep continuously on the radio module, that usually represents the highest power drain of the WSN node power budget. Synchronization strategies among the nodes have been also implemented in order to limit the on-time of the transceiver. The density of the *anchor nodes* depends both to the number of sensor nodes and to the dimension of the area to be monitored. Summarizing, the deployment of the network has to take into consideration multiple parameters that are optimized during the planning phase once the museum requirements and characteristics are known. Fig. 4.1 shows an example of the implemented hybrid architecture. The blue points represent the anchor nodes while the green ones are the sensor nodes. The control unit is the element of the network interconnected with the anchor nodes through a multi-hop strategy and in charge of collecting all the data acquired by sensor nodes. The control unit performs pre-processing tasks and stores data both locally and on a remote database for successive analysis.

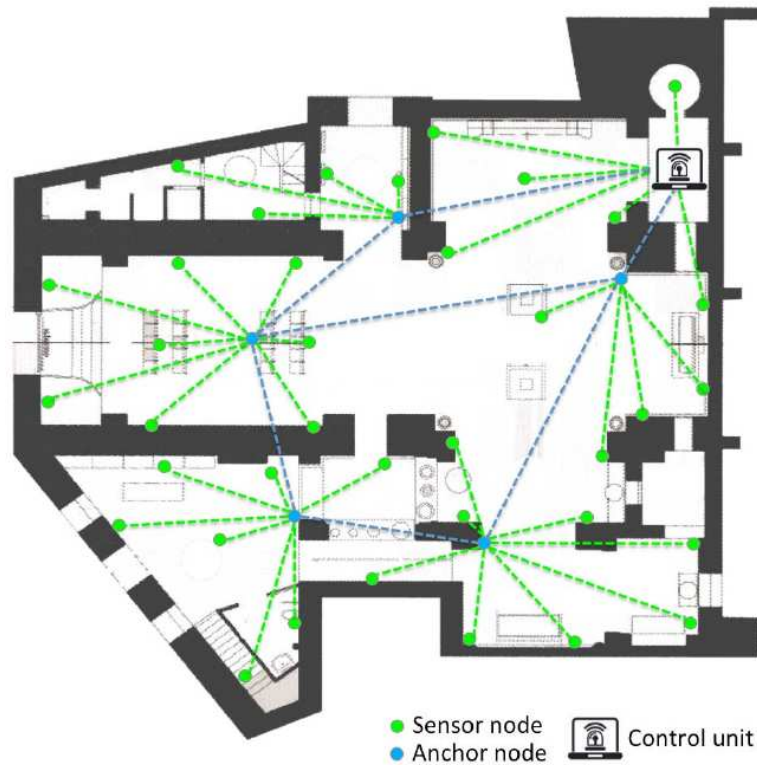


Figure 4.1: Hybrid WSN architecture for complex museum monitoring.

The museum scenario depicted in Fig. 4.1 presents the typical challenge of thick walls of historic buildings. This aspect has to be carefully considered during the network design process, in order to guarantee the right wireless communication of sensor nodes towards the closest anchor node. In addition, the typical low density (or absence) of power sockets in museums increases the complexity in the design of the monitoring system and forces the adoption of battery-powered *anchor nodes*, which integrate much more advanced power saving strategies to increase the system lifetime reducing as much as possible the maintenance interventions. Summarizing, museums can be reasonably considered complex scenarios in which wireless monitoring systems need to be carefully designed to guarantee high reliability and robustness. [80]

4.2 Control Strategy

We can consider a finite set of K WSN nodes positioned at known positions $r_k = (x_k, y_k, z_k)$, $k = 1, \dots, K$ inside a monitored threedimensional domain Ω (Fig. 4.2).

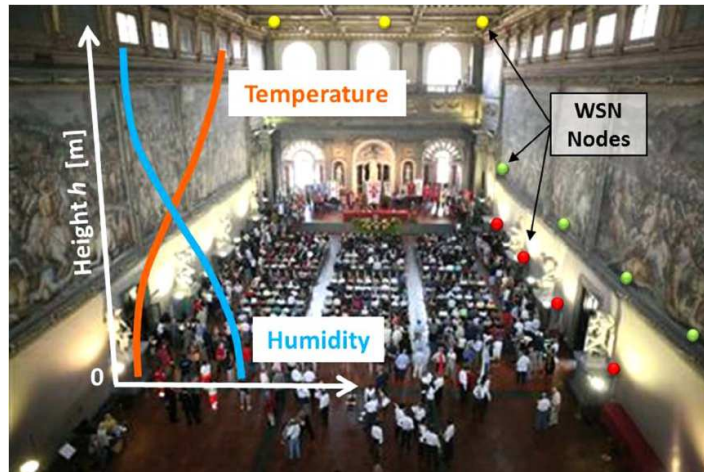


Figure 4.2: WSN deployment in a museum.

In each sensor node there are some environmental sensors for the acquisition of the features vector $\rho(r_k, t) \in \mathbb{R}^{F \times 1}$, where t is the sampling time-instant and F the number of environmental features. The sensor nodes acquire each feature and transmit them (e.g., the air temperature, the humidity, etc.) to the gateway node through multi-hop wireless connections, that will be finally saved in a remote database. The proposed algorithm runs on a remote control unit and its goal is to estimate the occupancy level $O_\Omega(t)$ of the domain Ω , which is defined as the percentage of the maximum number of people allowed within Ω according to the museum regulations, starting from the knowledge of the environmental feature vector. To this end, will be considered the following basic physical principles of indoor environmental behavior:

1. the hot air raises to the top when people occupy the domain Ω .
2. the humidity saturates from below when people occupy the domain Ω .

Let the WSN nodes be distributed so that $z_k \in [h_i, i = 1, \dots, I]$; $k = 1, \dots, K$, $h_1 < h_2 < \dots < h_I$ being the vertical positions of the nodes. Furthermore, let $\alpha(h, t)$ be the function describing the vertical profile of the temperature values, while $\beta(h, t)$ denotes the humidity profile function as shown in Fig. 4.3.

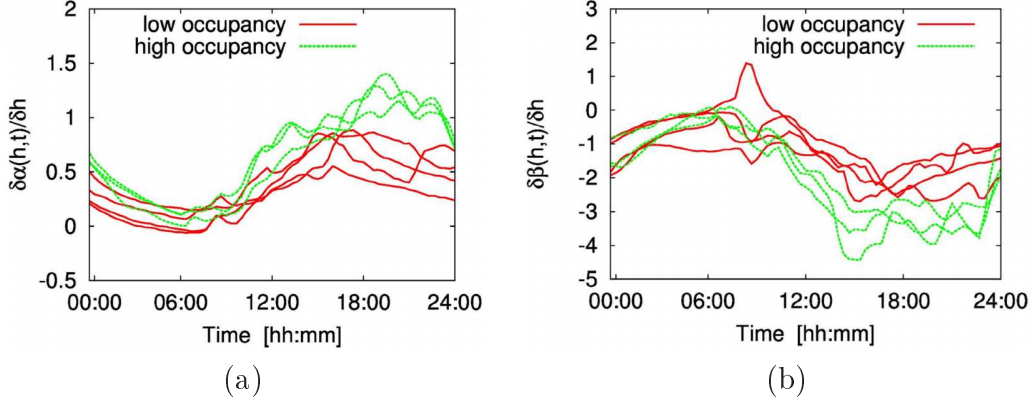


Figure 4.3: Vertical distributions of (a) the temperature profile $\alpha(h, t)$, and (b) the humidity profile $\beta(h, t)$.

By considering that there is a connection between the occupancy percentage and the slope of such distributions [i.e., a high occupancy causes an increase of the positive slope of a $\alpha(h, t)$ as well as a decrease of the negative slope of $\beta(h, t)$], the first derivatives of the corresponding vertical profiles have been evaluated to determine the so-called environmental occupancy indicator defined as

$$\Gamma(t) = \lambda \frac{\partial \alpha(h, t)}{\partial h} - \phi \frac{\partial \beta(h, t)}{\partial h} \quad (4.1)$$

where λ and ϕ are suitable calibration coefficients that balance the impact of the temperature and the humidity in each museum environment. Even if it is clear that $\Gamma(t)$ increases with the museum occupancy and it tends to zero when the domain is empty, the relation between $\Gamma(t)$ and the actual museum occupancy $O_\Omega(t)$ depends on multiple and time-varying conditions in a nonlinear fashion including the building characteristics and materials, the air management systems, and the external weather conditions, and so forth. Consequently, neither simple descriptive models can be adopted nor analytic closed-forms are available. The occupancy estimation problem at hand has then been addressed by recurring to the generalization capabilities of a learning-by-example strategy based on support vector machine (detailed explained in Sub-Section 4.2.1)[61]. More in detail, in this work has been adopted the support vector regression (SVR) to evaluate a linear regression function in a high dimensional feature space where the data are mapped through a nonlinear function $\Psi[\Gamma(t)] = O_\Omega(t)$. A finite set of R input-output learning patterns $(\Gamma(t), O_\Omega(t))_r; r = 1, \dots, R$ has been collected to train the SVR once and offline.

After the training phase, the SVR processes the available feature vectors $\rho(r_k, t)$ collected by the WSN nodes in real-time, calculates the environmental

indicator $\Gamma(t)$, and in the end provides the estimated occupancy level $\hat{O}_\Omega(t)$. [105]

4.2.1 Support Vector Machine

Learning-by-examples techniques are computer-aided approaches based on machine learning [88] that are pointed at solving complex real-world problems. In our case the “complexity” can be related to the need of computing the solution in real-time, not feasible by means of other methods. To address these problems, LBE strategies are characterized by two phases: the *training phase* and the *testing phase*.

- In the *training phase*, a LBE technique learns the behavior of a function from a set of input-output pairs. The goal of the training is the creation of a surrogate model able to emulate the real system.
- In the *testing phase*, the LBE technique is applied to input samples not observed during the training phase and is able to generalize what learned.

Support Vector Machine is a Learning-by-examples technique built on a solid theoretical framework, the statistical learning theory [89], in which the definition of the control parameters of $\underline{\varphi}(\bullet)$ is formulated as a quadratic optimization problem ensuring a global optimum. Moreover, the resulting model turns out being sparse, since only training samples associated to non-vanishing coefficients (i.e., the so-called “support vectors”) are exploited to make predictions, thus controlling the model complexity and avoiding over-fitting. [90]

The SVM-based classification approach can be formulated as the following two-step procedure[61]:

1. Determining a decision function $\hat{\Phi}$ that correctly classifies an input pattern $(\underline{\Gamma}, m)$ (not necessarily belonging to the training set);
2. Mapping the decision function $\hat{\Phi}\{(\underline{\Gamma}, m)\}$ into an *a posteriori* probability $Pr\{\underline{\chi} = \underline{1}|\underline{\Gamma}\}$.

4.2.1.1 Definition of the Decision Function

At this step, we define χ_m , $m = 1, \dots, M$ as the points of a two-dimensional space, which status will be determined by the algorithm. Mathematically, such a problem formulates in the definition of a suitable discriminant function $\hat{\Phi}$ separating the two classes, which are labeled as $\chi = +1$ and $\chi = -1$. Since these classes are nonlinearly separable, the definition of a non-linear (in terms of the original data $\underline{\Gamma}$) discriminant function is usually required as well as the solution of an optimization problem where multiple optima (also local optima) are present.

4.2. CONTROL STRATEGY

SVM defines a linear decision function corresponding to a hyperplane that maximizes the separating margin between the classes and it requires the solution of an optimization problem where only one minimum there exists. More in detail, the linear data-fitting is not carried out in the original input space $\mathfrak{R}\{\underline{\Gamma}\}$, but in a higher dimensional space $\mathfrak{R}\{\underline{\varphi}(\underline{\Gamma})\}$ (called *feature space*) where the original examples are mapped through a nonlinear operator, $\underline{\varphi}(\bullet)$. The nonlinear SVM classifier so obtained is defined as

$$\hat{\Phi}(\underline{\varphi}(\underline{\Gamma}, m)) = \underline{\omega} \cdot \underline{\varphi}(\underline{\Gamma}, m) + b \quad m = 1, \dots, M \quad (4.2)$$

where $\underline{\omega}$ and b are the parameters of $\hat{\Phi}$ to be determined during the training phase and $\underline{\varphi}(\underline{\Gamma}, m)$ is a non-linear function mapping the original input data, $(\underline{\Gamma}, m)$, to a higher dimensional space, called feature space, where the surrogate model can be defined through a simple linear function (4.2) (Fig. 4.4).

The hyperplane so-defined causes the largest separation between the decision function values for the “margin” training examples from the two classes. Mathematically, such a hyperplane can be found by minimizing the following cost function

$$\Omega(\underline{\omega}) = \frac{1}{2} \|\underline{\omega}\|^2 \quad (4.3)$$

subject to the separability constraints

$$\begin{aligned} \underline{\omega} \cdot \underline{\varphi}(\underline{\Gamma}^{(n)}, m) + b &\geq +1 \text{ for } \chi_m^{(n)} = +1, & m = 1, \dots, M \\ \underline{\omega} \cdot \underline{\varphi}(\underline{\Gamma}^{(n)}, m) + b &\leq -1 \text{ for } \chi_m^{(n)} = -1, & n = 1, \dots, N \end{aligned} \quad (4.4)$$

In this sense, SVM can be considered as a kind of regularized network, as indicated in [91].

However, since the training data in the feature space are generally noncompletely separable by a hyperplane, *slack variables* (denoted by $\xi_{(m)}^{(n)}$) are introduced to relax the separability constraints in (4.4) as follows:

$$\begin{aligned} \underline{\omega} \cdot \underline{\varphi}(\underline{\Gamma}^{(n)}, m) + b &\geq 1 - \xi_{(m)+}^{(n)} \text{ for } \chi_m^{(n)} = +1, & m = 1, \dots, M \\ \underline{\omega} \cdot \underline{\varphi}(\underline{\Gamma}^{(n)}, m) + b &\leq \xi_{(m)-}^{(n)} - 1 \text{ for } \chi_m^{(n)} = -1, & n = 1, \dots, N \end{aligned} \quad (4.5)$$

Such a procedure is justified by the Cover’s theorem, a key point in the SVM methodology as indicated in [92].

Thus, the cost function in (4.3) turns out to be

$$\Omega(\underline{\omega}) = \frac{\|\underline{\omega}\|^2}{2} + \frac{C}{\sum_{m=1}^M \{N_{(m)}^- + N_{(m)}^+\}} \times \sum_{m=1}^M \left\{ \sum_{n=1}^{N_{(m)}^+} \xi_{(m)+}^{(n)} + \sum_{n=1}^{N_{(m)}^-} \xi_{(m)-}^{(n)} \right\} \quad (4.6)$$

where $N_{(m)}^+$ and $N_{(m)}^-$ indicate the number of training patterns for which $\chi_m^{(n)} = +1$ and $\chi_m^{(n)} = -1$, respectively. The user-defined hyperparameter C controls the tradeoff between the *empirical risk* (i.e., the training errors) and the model

complexity [the first term in (4.7)] to avoid the *overfitting*. In that case, the decision boundary too precisely corresponds to the training data. Thereby, the method is unable to deal with data outside the training set [92].

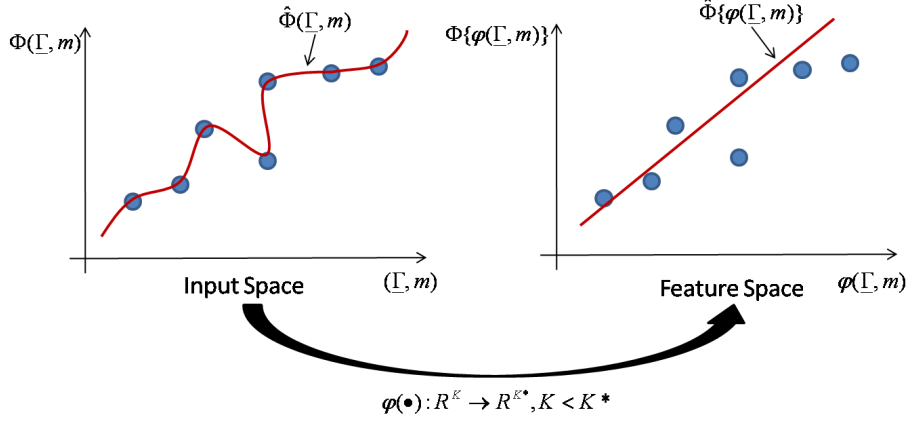


Figure 4.4: Non-linear mapping of the input space to the feature space.

Moreover, to include a priori knowledge about class distributions [93], two weighting constants can be defined $\lambda_+ = C / \sum_{m=1}^M N_{(m)}^+$ and $\lambda_- = C / \sum_{m=1}^M N_{(m)}^-$ [94], and (4.6) modifies as follows:

$$\Omega(\underline{\omega}) = \frac{\|\underline{\omega}\|^2}{2} + \lambda_+ \sum_{m=1}^M \sum_{n=1}^{N_{(m)}^+} \xi_{(m)}^{(n)} + \lambda_- \sum_{m=1}^M \sum_{n=1}^{N_{(m)}^-} \xi_{(m)}^{(n)-} \quad (4.7)$$

In order to minimize (4.7), it can be observed that a necessary (4.3) condition is that is a linear combination of the mapped vectors $\underline{\varphi}(\underline{\Gamma}^{(n)}, m)$

$$\underline{\omega} = \sum_{m=1}^M \sum_{n=1}^N \left\{ \alpha_m^{(n)} \chi_m^{(n)} \underline{\varphi}(\underline{\Gamma}^{(n)}, m) \right\} \quad (4.8)$$

where $\alpha_m^{(n)} \geq 0$, $n = 1, \dots, N$, $m = 1, \dots, M$ are Lagrange multipliers to be determined. Moreover, from the Karush-Khun-Tucker conditions at the optimality [95], b turns out to be expressed as follows:

$$b = \frac{\sum_{m=1}^M \sum_{n=1}^{N_{sv}} \left\{ \chi_m^{(n)} - \sum_{q=1}^M \sum_{p=1}^N \left\{ \alpha_m^{(p)} \underline{\varphi}(\underline{\Gamma}^{(n)}, m) \cdot \underline{\varphi}(\underline{\Gamma}^{(p)}, q) \right\} \right\}}{N_{sv}} \quad (4.9)$$

N_{sv} being the number of patterns $(\underline{\Gamma}^{(n)}, m)$ for which $\alpha_m^{(n)} \neq 0$ (called *support vectors*). Since support vectors lie on the hyperplane for which (4.5) is satisfied

4.2. CONTROL STRATEGY

with equality, they are taken into account for the classification while the others are neglected. Such an event reflects the “sparsity” property of the SVM classifier allowing the use of few input patterns. Substituting (4.8) and (4.9) in (4.2) yields

$$\begin{aligned} \hat{\Phi}(\underline{\varphi}(\underline{\Gamma}), m) &= \sum_{m=1}^M \sum_{n=1}^N \left\{ \alpha_m^{(n)} \chi_m^{(n)} \Theta \left(\underline{\Gamma}^{(n)}, \underline{\Gamma}, p, m \right) \right\} + \\ &+ \frac{\sum_{m=1}^M \sum_{n=1}^{N_{sv}} \left\{ \chi_m^{(n)} - \sum_{q=1}^M \sum_{p=1}^N \left\{ \alpha_m^{(p)} \Theta \left(\underline{\Gamma}^{(n)}, \underline{\Gamma}^{(p)}, p, m \right) \right\} \right\}}{N_{sv}} \end{aligned} \quad (4.10)$$

where $\Theta \left(\underline{\Gamma}^{(i)}, \underline{\Gamma}^{(j)}, p, m \right) = \underline{\varphi}(\underline{\Gamma}^{(i)}, p) \cdot \underline{\varphi}(\underline{\Gamma}^{(j)}, m)$ is a suitable *kernel function* [96]. Then, the decision function is completely determined when the Lagrange multipliers are computed. Toward this end, the constrained optimization problem formulated in (4.6) and (4.5) is reformulated in a more practical dual form. The solution of the dual problem, which is equivalent to the solution of the primal optimization problem (4.3)-(4.4), appears in (4.11), subject to $\sum_{n=1}^N \sum_{m=1}^M \alpha_m^{(n)} \chi_m^{(n)} = 0$, $\alpha_m^{(n)} \in [0, \lambda_-]$ if $\chi_m^{(n)} = -1$ and $\alpha_m^{(n)} \in [0, \lambda_+]$ otherwise.

$$\begin{aligned} &max_{\underline{\alpha}} \{ \Omega_{Dual}(\underline{\alpha}) \} = \\ &= max_{\underline{\alpha}} \left\{ \frac{\sum_{n=1}^N \sum_{p=1}^N \sum_{m=1}^M \sum_{q=1}^M \left[\alpha_m^{(n)} \alpha_q^{(p)} \chi_m^{(n)} \chi_q^{(p)} \Theta \left(\underline{\Gamma}^{(n)}, \underline{\Gamma}^{(p)}, p, m \right) \right]}{2} - \right. \\ &\quad \left. - \sum_{m=1}^M \sum_{n=1}^N \alpha_m^{(n)} \right\} \end{aligned} \quad (4.11)$$

Finally, since $\Omega_{Dual}(\underline{\alpha})$ is a convex and quadratic function of the unknown parameters $\alpha_m^{(n)}$, it is solved numerically by means of a standard quadratic programming technique (e.g., the Platt’s SMO algorithm for classification [97], an optimal implementation of the SMO algorithm is the “LibSVM” tool available at <http://www.kernel-machines.org>). More in detail, the SMO algorithm breaks the large optimization problem at hand in a series of smaller ones characterized by only two variables and solved through an effective updating formula [97], thus inducing nonnegligible computational savings. [61]

4.2.1.2 Mapping of the Decision Function Into the A Posteriori Probability

Concerning standard classification, the SVM classifier labels an input pattern according to the following rule [98]:

$$\chi_m = sign \left\{ \hat{\Phi}(\underline{\varphi}(\underline{\Gamma}, m)) \right\}, \quad m = 1, \dots, M \quad (4.12)$$

Unlike standard approaches, the proposed method is aimed at defining an a *posteriori* probability. Consequently, some modifications to the standard SVM-based classification approach are needed. Toward this aim, a set of efficient

solutions has been proposed (e.g., see [96], [99]-[101]) either based on a direct training of the SVM with a logistic link function and a regularized maximum-likelihood score or based on a *posterior* fitting probability process.

The first class of approaches usually leads to nonsparse kernel machines and requires a significant modification of the SVM structure. In this paper, the *a posteriori* probability fitting method [101] is adopted since the use of a parametric model allows a direct fitting of the *a posteriori* probability $Pr\{\underline{\chi} = \underline{1}|\underline{\Gamma}\}$. More in detail, such a model approximates the *a posteriori* probability through a sigmoid function

$$Pr\{\chi_m = 1|(\underline{\Gamma}, m)\} = \frac{1}{1+\exp\{\gamma\hat{\Phi}(\underline{\varphi}(\underline{\Gamma}, m)+\delta)\}}, \quad m = 1, \dots, M \quad (4.13)$$

where γ and δ are unknown parameters to be determined.

To estimate the optimal values for the parameters of the sigmoid function, a fitting process is performed. A subset of the input patterns of the training set is chosen $\{(\underline{\Gamma}, m, \chi_m; m = 1, \dots, M)^{(s)}; s = 1, \dots, S\}$, where $\hat{\Phi}_m^{(s)} = \hat{\Phi}(\underline{\varphi}(\underline{\Gamma}^{(s)}, m))$. Then, the following cost function is defined as in (4.14) and successively minimized to define γ and δ according to the numerical procedure proposed by Lin et al. (see <http://www.csie.ntu.edu.tw/~cjlin/>,) to solve the problems (i.e., the use of a kind of Levenberg-Marquardt method for unconstrained optimization) of the implementation of Platt's probabilistic outputs method pointed out in [101].

$$\begin{aligned} \Upsilon(\gamma, \delta) = & - \sum_{s=1}^S \sum_{m=1}^M \left\{ \frac{\chi_m^{(s)}+1}{2} \log \left[\frac{1}{1+\exp(\gamma\hat{\Phi}_m^{(s)}+\delta)} \right] + \right. \\ & \left. + \left(\frac{1-\chi_m^{(s)}}{2} \right) \log \left[\frac{\exp(\gamma\hat{\Phi}_m^{(s)}+\delta)}{1+\exp(\gamma\hat{\Phi}_m^{(s)}+\delta)} \right] \right\} \end{aligned} \quad (4.14)$$

Summarizing, the SVM optimization problem needs three successive steps:

1. determining the hyperparameters array (*model selection*), i.e., C and all the parameters that define the kernel function (e.g., the Gaussian σ^2 width when Gaussian kernels are used), by considering the “*training dataset*”;
2. determining the *functional parameters* $\underline{\alpha}$ and b starting from the “*training dataset*” and solving the dual problem (4.11);
3. determining the *a posteriori fitting parameters* γ and δ starting from a subset of the “*training dataset*” (validation phase);
4. testing the SVM on a different dataset (*test phase*).

[61]

4.3 Experimental Validation and Results

The main objective of museums is to make artworks accessible to the public and at the same time to ensure the longterm safety and preservation of the collections. In the past, chart recorders and hygrothermographs were the most common instruments used to monitor various areas within a museum, but this is rapidly changing in the last years. With the diffusion of digital monitoring devices, alternatives such as data loggers are more and more widely adopted. Digital solutions minimize maintenance tasks, like the regular change of charts and the manual calibration performed by trained staff. However, even if such solutions represent an advance respect to analog recording devices, they still present many limitations with respect to the emerging needs of museums that will go beyond the environment monitoring. Indeed, the current trend is to enhance the connection of the museum with its audience, so that the visitors' preferences can be exploited to provide additional "personalized" services [104]. The experimental validation of a WSN-based infrastructure for the monitoring of museum environment is presented. The hardware platform has been designed and realized for the deployment in the "Sala dei 500", the most important chamber inside the Palazzo Vecchio, Florence, Italy. The network of sensors acquires heterogeneous data, starting from the environmental parameters, with the aim of reproducing the museum characteristics through web-based application tools and enhancing the interactions between museum and users. The software architecture has been developed to enable the integration of additional services based on the collection of sensor data eventually fused together with other available museum information. The installation of the system in a highly visited museum has given the opportunity to test the capabilities and robustness of the WSN technology in dealing with the monitoring of large and crowded spaces. The details of the installation and the preliminary obtained results are here reported as a representative test case of the E-Museum platform validation. [103]

4.3.1 WSN Node Prototype

The prototypes of sensor node and anchor node typologies have been realized integrating the transmitting/receiving unit, the antenna, the power subsystem, the computational unit, and the sensors within a small package of maximum size 90x65x25 mm. The dimensions have been reduced as much as possible to limit the visual impact in the proximity of the artworks. Fig. 4.5 shows a prototype of a sensor node that integrates a temperature and humidity sensor, with accuracy $\pm 0.3^{\circ}\text{C}$, $\pm 2\%\text{RH}$ in the range -40°C , $+125^{\circ}\text{C}$ and $0-100\%\text{RH}$, a light sensor sensible to light wavelength in the range 430-1100 nm, and finally a three-axes accelerometer, with $\pm 1.5\text{g}$ sensitivity.



Figure 4.5: Prototype of the WSN sensor node.

The sensor unit can be easily modified and integrated thanks to the available expansions that has been made available on the main hardware platform (up to 15 digital I/O lines and 4 12bit-ADC available for additional sensors). As an example, high-precision thermistors for surface temperature measurements as well as light sensors for UV radiation measurements have been designed for successive integration.

The radio module is compliant to IEEE 802.15.4 low-power standard, using the sub-GHz reference working frequency $f=868$ MHz. This frequency guarantees better propagation throughout the museum rooms respect to the widely diffused 2.4GHz ISM frequency band. Good coverage performance are also guaranteed by the maximum transmitting power that can be dynamically configured (up to $P_{tx}=12$ dBm) and by the very high receiver sensitivity (down to $S_{rx}=-121$ dBm).

Once the devices have been installed, the remote control of the wireless network allows direct control of every single WSN node, that can be configured in real-time according to the museum staff expertise. The maintenance of the nodes is minimized since information about the hardware and battery status are given only if an action is required. The battery lifetime strictly depends by the transmission rate. Assuming a time delay of 10 minutes between two successive transmissions, the duration is around 13-15 months using standard AA commercial batteries.

4.3.2 Deployment in a Real Museum Environment

The WSN nodes have been deployed in museum areas according to curators suggestions in order to guarantee representative data measurements from the preservation point of view. The high flexibility of the wireless infrastructure has been fully exploited since most of the measurement points are usually very difficult to reach and the quality of the wireless connections has been guaranteed through the adaptive management of multihop network topology. Each wireless node is equipped with a multi-sensor platform for the measurement of the desired parameters. Both temperature and relative humidity sensors are integrated in the designed board. All the sensor data are measured through analog to digital converters and locally stored for pre-processing before the transmission throughout the wireless network. Power saving strategies have been carefully implemented on-board in order to limit as much as possible the consumptions related both to the sensors and the radio transceiver.

The implemented network allows bidirectional communications between the nodes and the remote control unit. Respect to standard WSN infrastructures that enable only one-way data collection from the sensors to the gateway, the proposed system provides a set of commands (e.g., on-off, calibration, diagnostic commands) that the end-user can use to interrogate a specific node or a set of nodes. The acquired data are collected by a control unit dedicated to data processing and storage. Data fusion strategies have been implemented to generate an aggregated representation of the monitored domain. A user-friendly web tool (Fig. 4.6) has been developed to enable both data visualization and interaction with the system.

The proposed E-Museum monitoring system has been deployed in the “Sala dei 500”, inside Palazzo Vecchio, the town hall of Florence, Italy, (Fig. 4.7) that represents one of the most significant public spaces in Italy. The “Sala dei 500” has a length $L=52\text{m}$ and width $W=23\text{m}$. The ceiling, that is adorned with 39 panels, is $H=18\text{m}$ high. A set of $N=22$ wireless nodes has been installed at different heights according to the monitoring requirements (Fig. 4.8).

CHAPTER 4. OPPORTUNISTIC OCCUPANCY ESTIMATION SYSTEM
FOR MUSEUM ENVIRONMENTS

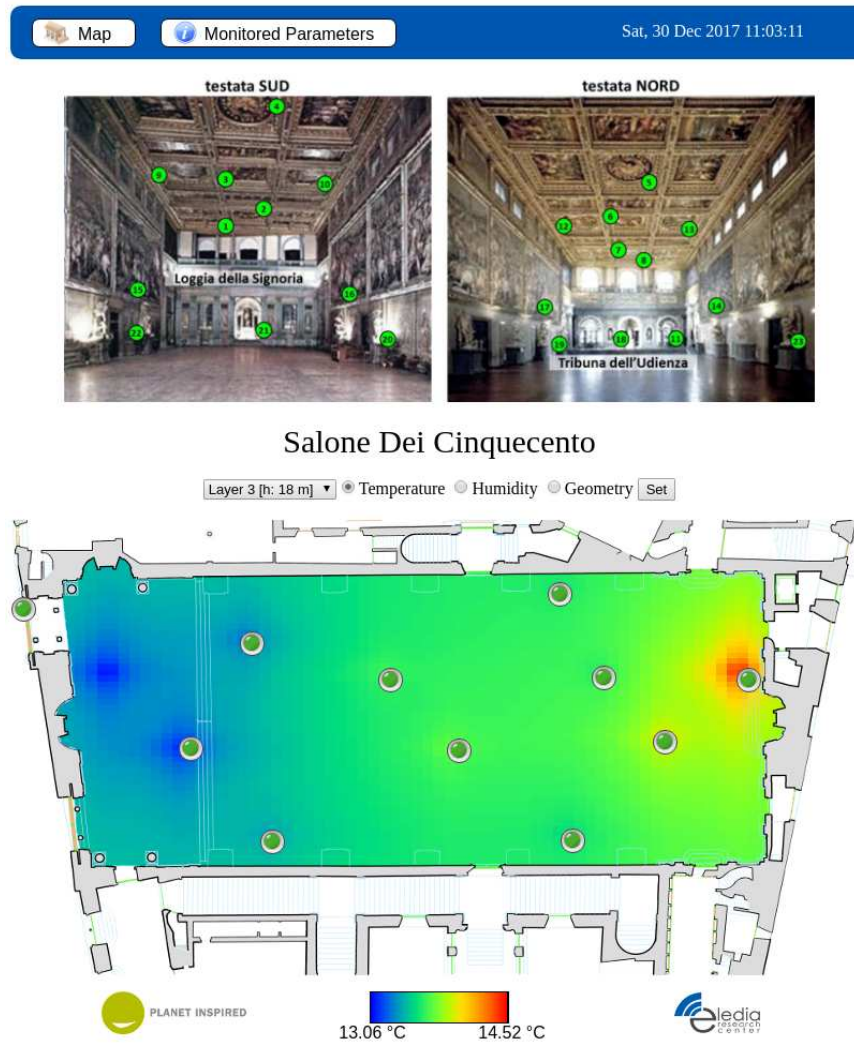


Figure 4.6: EMuseum Web Tool.

4.3. EXPERIMENTAL VALIDATION AND RESULTS



(a)



(b)



(c)



(d)



(e)



(f)

Figure 4.7: Network Installation inside the “Sala dei 500”.

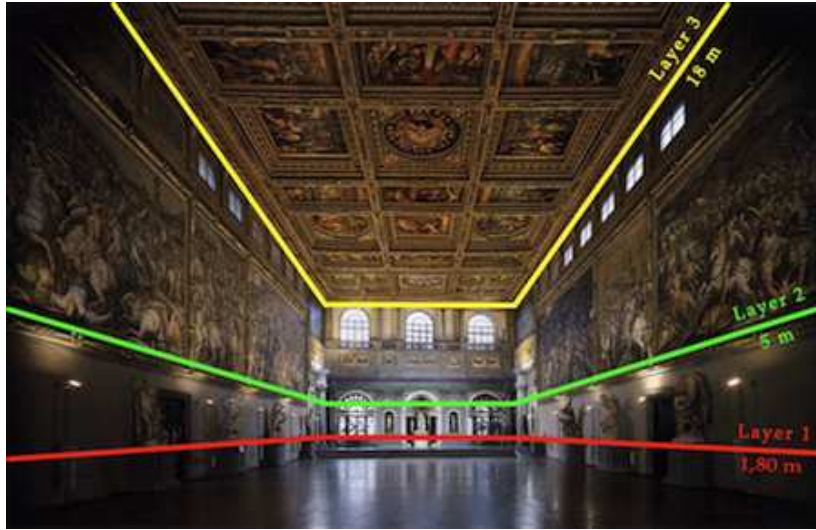


Figure 4.8: Sensing layers inside the “Sala dei 500”.

In particular, three horizontal layers have been identified at the heights $h_1 = 1.8$ m, $h_2 = 5.0$ m, and $h_3 = 18$ m, close to the sculptures, the wall paintings, and the paneled ceiling, respectively. Moreover, an additional node has been installed outdoor [Fig. 4.7(f)], on the building side close to Piazza della Signoria, for indoor-outdoor correlation. The installation procedures have been carried out in collaboration with the trained staff of the museum. In particular, the nodes at height h_3 have been hanged with hand-line and raised up from the upper side of the paneled ceiling where only authorized technicians have access. Finally, the sensors have been positioned as close as possible to the target artworks. Once all the sensors have been installed, the boot sequence has been executed through the implemented user commands in order to activate the acquisition with the desired time interval. The graphical interface of the E-Museum web tool has been activated in order to visualize the processed data and to enable the interaction with all the online sensors. Diagnostic information like battery status, internal CPU temperature, and wireless link quality can be requested (Fig. 4.9).

In case of node malfunctioning or discharge, automatic messages are sent to the control unit in order to plan the maintenance. Thanks to the data storage in remote databases, even complex analysis of the historic data can be performed offline (Fig. 4.10). [103]

4.3. EXPERIMENTAL VALIDATION AND RESULTS



Figure 4.9: WSN Node Diagnostic Information.

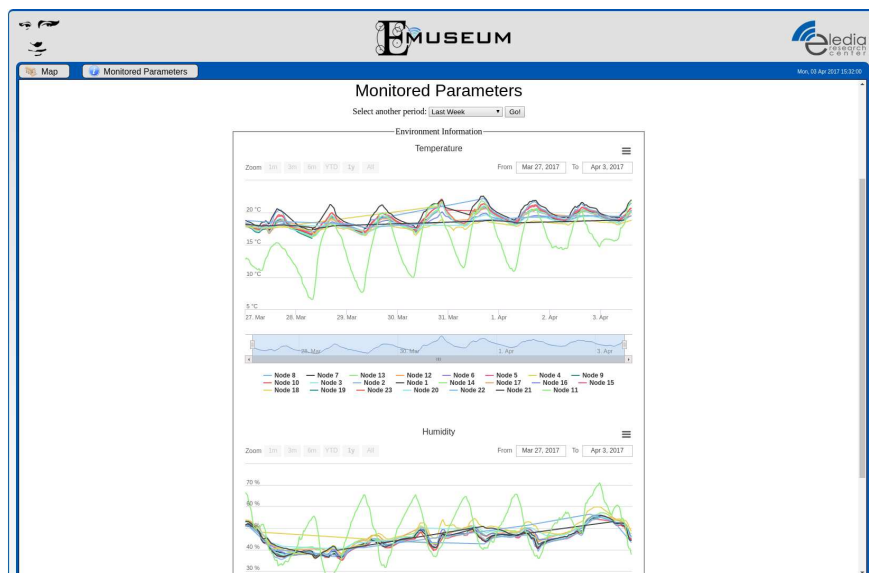


Figure 4.10: WSN Node Historic Data.

4.3.3 Occupancy Estimation

In the following will be presented a selected set of experimental results to show the potentialities and the limitations of the proposed occupancy estimation algorithm. The scenario is composed by the WSN described before: $K = 22$ nodes installed at $I = 3$ different heights, and each node is equipped with environmental sensors able to measure $F = 2$ features: the temperature and the humidity values. After the acquisition, the environmental information are sent with a sampling period of $\Delta t = 10'$; the optimal trade-off between the WSN power consumption and the necessary time-resolution for detecting the environmental variations.

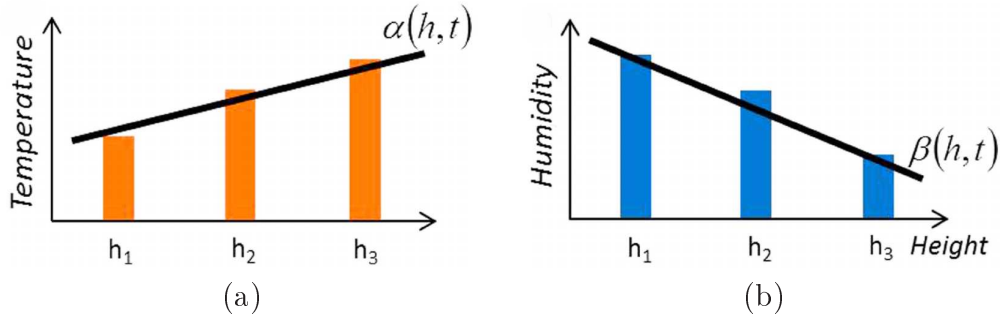


Figure 4.11: Derivatives of daily vertical profiles of (a) the temperature, and (b) the humidity.

For illustrative purposes, Fig. 4.11 shows the first derivative of the vertical profile of the temperature [Fig. 4.11(a)] and the humidity [Fig. 4.11(b)] for different occupancy conditions (low and high). As it can be experimentally proved and observed, large values of $\frac{\partial \alpha(h,t)}{\partial h}$ and small values of $\frac{\partial \beta(h,t)}{\partial h}$ occur at the same time when the domain occupancy is high.

As for the environmental occupancy indicator $\Gamma(t)$, it has been determined by applying (4.1) and setting the calibration parameters to $\phi = 0.5$ and $\lambda = 0.5$. Regarding the estimation of the occupancy index $\hat{O}_\Omega(t)$, radial basis kernel functions have been chosen for the SVR-based method trained with a set of $r = 1008$ known input-output data, that correspond to one week of acquisitions, and setting the SVR metaparameters to $\varepsilon = 0.1$ and $c = 10$. Later, the experimental prediction has been performed with unknown (i.e., input data not belonging to the training set) test data related to three representative situations:

1. closed museum;
2. normal week-day;

4.3. EXPERIMENTAL VALIDATION AND RESULTS

3. crowded museum during a special event.

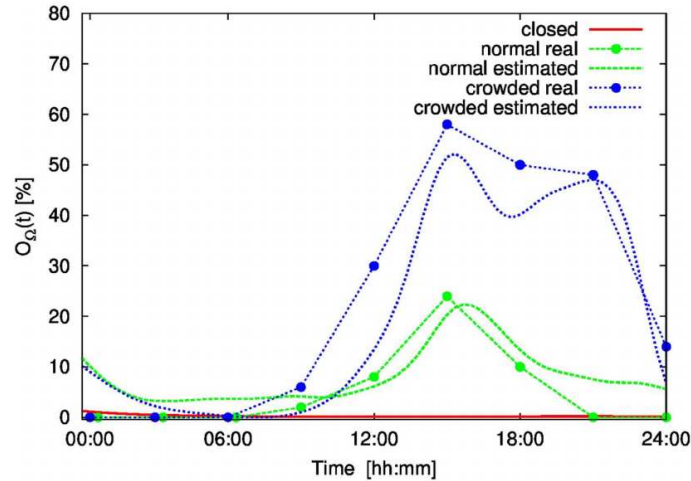


Figure 4.12: Actual and estimated indoor occupancy.

Fig. 4.12 represents the estimated occupancy levels and the real occupancy trends as inferred from the museum ticketing. The comparison underlines that there is a good matching between estimated and real occupancy percentages in any. As expected, there is a shift between the estimated trends and the actual occupancy due to the time-delay of the environmental indexes in "recognizing" the variations of the people presence. In reverse, this latter can be easily avoided considering it during the training phase.

As expected, there is a shift between the estimated trends and the actual occupancy due to the time-delay of the environmental indexes in "recognizing" the variations of the people presence. In reverse, this latter can be easily avoided considering it during the training phase. [105]

Chapter 5

Conclusions

In this Chapter, conclusions and future developments regarding the proposed system are presented. In particular, additional considerations are given regarding the actual status of these systems.

5.1 Conclusions and Future Developments

In this thesis, innovative wireless solutions for the development of smart environments have been proposed. Adaptive, learning, cognitive and bio-inspired systems as well as distributed and embedded control and sensing have been studied, and tested as an important avenue for the medium to long term development of the next-generation smart cities. Each solution has been developed starting from the combination of wireless platforms with dedicated data analysis methods to enable not only the data acquisition, but also the adaptive decision support according to the real end-users needs in different applicative scenarios. The selected systems have been experimentally validated in real test-sites to point out the real-world applicability of the proposed wireless solutions.

Going into detail, this thesis has presented systems that belong to the so-called smart cities and smart building.

The concept of smart cities has been applied in power management, with a wireless distributed system for smart public light management. A demonstrative prototype composed by more than 700 controlled lamps has been installed in the city of Trento, Italy, for the experimental assessment of the advantages and limitations of the investigated solution. The introduction of adaptive dimming profiles calibrated according to the time varying conditions of the scenario has enabled a total energy saving close to 30 [%] after a three-years measurement campaign. The optimization of the dimming rules may offer even higher performance and future activities will be also focused on the integration of smart methods for the automatic and real-time calibration of the rules to support the decisions of the operators in the smart lighting system management.

On the other hand, the concept of smart building has been treated describing smart monitoring systems of indoor areas with wireless sensors. Particular attention has been given to the monitoring of museums as well as smart buildings such as residential homes. First of all the energy saving problem in smart buildings has been re-elaborated as a multiplayer game and an appropriate strategy based on game theory has been implemented in a Decision Support System, that helps the end user to choose the best time slot to switch on his appliances. The proposed system has been preliminary assessed through both experimental and numerical tests showing good performance in reducing the energy costs and *PAR* (Peak to Average Ratio). Later, the energy saving problem has been applied to a different scenario, the intelligent control of lightning in a smart museum. In this specific context, there are multiple goals: increase the visitor experience quality and minimize the power consumption of the lighting system. This system is composed of a Wireless Sensor and Actuator Network (WSAN) that acquires light and power quantities from the environment and controls the lamp intensity in order to reach the goals of this system. The control strategy is based on a Particle Swarm Optimizer (PSO) that minimizes a multi-term cost function. The obtained results point out the capability to find the optimal actuation strategy

able to satisfy the constraints on both energy saving (up to 37%) and the quality of the artworks presentation (for more than 95% of the considered time). Finally, the environment of the smart museum has been treated, by proposing a system for the monitoring of environmental parameters in order to safeguard the status of artwork, using the WSN technology. Taking advantage of environmental information available from a WSN devoted to artwork conservation purposes, an occupancy estimation algorithm has been implemented. By exploiting the generalization properties of a suitably trained SVR-based strategy, the evaluation of the complex relation between visitors occupancy and environmental parameters has been performed and preliminary evaluated in a real-world experimental setup (Sala dei 500, Firenze, Italy). The obtained results have confirmed the potentialities of the proposed approach for improving the awareness on the museum usage, the museum quality-of-service, and the security issues related to the flow management.

5.1. CONCLUSIONS AND FUTURE DEVELOPMENTS

Bibliography

- [1] M. Weiser, "The computer for the 21st century," *Scientific Am.*, vol. 265, no. 3, pp. 94-104, Sep. 1991.
- [2] F. Viani, P. Rocca, G. Oliveri, and A. Massa, "Pervasive remote sensing through WSNs," *6th European Conference on Antennas and Propagation 2012 (EUCAP2012)*, Prague, March 26-30, 2012.
- [3] M. Benedetti, L. Ioriatti, M. Martinelli, and F. Viani, "Wireless sensor network: a pervasive technology for earth observation," in *IEEE Journal of Selected Topics in App. Earth Obs. And Remote Sens.*, vol. 3, no. 4, pp. 488-497, 2010.
- [4] J. K. Hart and K. Martinez, "Environmental sensor networks: A revolution in the earth system science?," *Earth-Science Reviews*, vol. 78, pp. 177-191, 2006.
- [5] M. Kuorilehto, M. Hannikainen, and T. D. Hamalainen, "A survey of application distribution in wireless sensor network," *EURASIP J. Wireless Commun. Netw.*, vol. 5, pp. 774-788, 2005.
- [6] I. F. Akyildiz, W. Su, Y. Sankarasubramaniam, and E. Cayirci, "Wireless sensor networks: A survey," *Computer Networks*, vol. 38, pp. 393-422, 2002.
- [7] F. Xia, Y.-C. Tian, Y. Li, and Y. Sun, "Wireless sensor/actuator network design for mobile control applications," *Sensors*, pp. 2157-2173, 2007.
- [8] B. Warneke, M. Last, B. Liebowitz, and K. S. J. Pister, "Smart dust: Communicating with a cubic-millimeter computer," *IEEE Computer*, vol. 34, pp. 44-51, Jan. 2001.
- [9] S. A. Shockfish, TinyNode 584 Embedded Wireless Network Node, TinyNode Fact Sheet [Online]. Available: <http://mail.millennium.berkeley.edu/pipermail/tinyos-2.0wg/attachments/20050316/ea40b043/sh-tn584-103-0001.pdf>
- [10] M. Gad-El-Hak, The MEMS Handbook. *New York: CRC Press*, 2002.

BIBLIOGRAPHY

- [11] S. S. Sonavane, V. Kumar, and B. P. Patil, "Designing wireless sensor network with low cost and low power," in *IEEE Int. Conf. Networks (ICON 2008)*, pp. 1-5, Dec. 12-14, 2008.
- [12] E. H. Callaway, *Wireless Sensor Networks-Architectures and Protocols*. Boca Raton, FL: Auerbach Publications, 2004.
- [13] M. M. Tentzeris and Y. Kawahara, "Novel energy harvesting technologies for ICT applications," in *Proc. Int. Symp. Applications and the Internet (SAINT 2008)*, pp. 373-376, Jul. 1, 2008.
- [14] A. Shrestha and L. Xing, "A performance comparison of different topologies for wireless sensor networks," in *Proc. IEEE Conf. Technologies for Homeland Security*, pp. 280-285, May 16-17, 2007.
- [15] F. Viani, F. Robol, M. Salucci, E. Giarola, S. De Vigili, M. Rocca, F. Boldrini, G. Benedetti, and A. Massa, "WSN-based early alert system for preventing wildlife-vehicle collisions in Alps regions - From the laboratory test to the real-world implementation," *EuCAP 2013*, Gothenburg, Sweden, pp. 1857-1860, April 8-12, 2013.
- [16] F. Viani, F. Robol, A. Polo, and E. Giarola, "Wildlife road-crossing monitoring system: Advances and test site validation," *10th European Conference on Antennas and Propagation (EUCAP 2016)*, Davos, Switzerland, pp. 1-4, April 11-15, 2016.
- [17] M. Rutishauser, V.V. Petkov, T. Williams, C. Wilmers, J. Boice, K. Obraczka, and P. Mantey, "CARNIVORE: A disruption-tolerant system for studying wildlife," in *Proc. of 19th Int'l Conf. on Computer Communications and Networks*, 2010, pp. 1-8.
- [18] J-H. Huang, Y-Y. Chen, Y-T. Huang, P-Y. Lin, Y-C. Chen, Y-F. Lin, S- C. Yen, P. Huang, and L-J. Chen, "Rapid prototyping for wildlife and ecological monitoring," *IEEE Systems Journal*, vol. 4, no. 2, pp. 198-209, 2010.
- [19] B. Wietrzyk and M. Radenkovic, "Energy efficiency in the mobile ad hoc networking approach to monitoring farm animals," *IEEE Int. Conf. on Networking and Services*, July 19-21, Silicon Valley, CA, USA, 2006.
- [20] F. Viani, A. Polo, F. Robol, A. Ferro, and E. Giarola, "Experimental validation of a wireless distributed system for smart public lighting management," *Proc. 2016 IEEE International Smart Cities Conference (ISC2)*, Trento, Italy, pp. 1-6, September 12-15, 2016.
- [21] T.M. Chen, "Smart grids, smart cities need better networks," *IEEE Network*, vol. 24, no. 2, pp. 2-3, 2010.

- [22] M. Naphade, G. Banavar, C. Harrison, J. Paraszczak, and R. Morris, "Smart cities and their innovation challenges," *Computer*, vol. 44, no. 6, pp. 32-39, 2011.
- [23] A. Ipakchi and F. Albuyeh, "Grid of the future," *IEEE Power and Energy Mag.*, vol. 7, no. 2, pp.52-62, 2009.
- [24] A study on saving energy in artificial lighting by making smart use of wireless sensor networks and actuator," *IEEE Network*, vol. 23, no. 6, pp. 16-20, 2009.
- [25] F.J.B. Outeirino, F. Domingo-Perez, A. del Rocio, J. F. Arias, and A. Moreno-Munoz, "In-building lighting management system with wireless communications," *IEEE Int. Conf. on Consumer Electronics*, pp. 83-85, 2012.
- [26] D. Han and J. Lim, "Smart home energy management system using IEEE 802.15.4 and Zigbee," *IEEE Trans. On Consumer Electron.*, vol. 56, no. 3, pp. 1403-1410, 2010.
- [27] P. Rocca, M. Benedetti, M. Donelli, D. Franceschini, and A. Massa, "Evolutionary optimization as applied to inverse problems," *Inverse Problems*, vol. 25, 123003, pp. 1-41, Dec. 2009.
- [28] J. Riha, Home automation trends, Diy Network. [Online]. Available: <http://www.diynetwork.com>.
- [29] M. R. Alam, M. B. I. Reaz, and M. Ali, "A review of smart homesVPast, present, an future," *IEEE Trans. Syst. Man Cybern. C, Appl. Rev.*, vol. 42, no. 6, pp. 1190-1203, Nov. 2012.
- [30] V. C. Gungor, D. Sahin, T. Kocak, S. Ergut, C. Buccella, C. Cecati, and G. P. Hancke, "Smart grid and smart homes: Key players and pilot projects," *IEEE Ind. Electron. Mag.*, vol. 6, no. 4, pp. 18-34, Dec. 2012.
- [31] S. Helal, C. Chen, E. Kim, R. Bose, and C. Lee, "Toward an ecosystem for developing and programming assistive environment," *Proc. IEEE*, vol. 100, no. 8, pp. 2489-2504, Aug. 2012.
- [32] T. J. Lui, W. Stirling, and H. O. Marcy, "Get smart," *IEEE Power Energy Mag.*, vol. 3, no. 3, pp. 66-78, Jun. 2010.
- [33] N. Langhammer and R. Kays, "Performance evaluation of wireless home automation networks in indoor scenarios," *IEEE Trans.*
- [34] J. Han, C.-S. Choi, and I. Lee, "More efficient home energy management system based on ZigBee communication and infrared remote controls," *IEEE Trans. Consumer Electron.*, vol. 57, no. 1, pp. 85-89, Feb. 2011.

BIBLIOGRAPHY

- [35] M. Dong, P. C. M. Meira, W. Xu, and W. Freitas, "An event window based load monitoring technique for smart meters," *IEEE Trans. Smart Grid*, vol. 3, no. 2, pp. 787-796, Jun. 2012.
- [36] F. G. Marmol, C. Sorge, O. Ugus, and G. M. Perez, "Do not snoop my habits: Preserving privacy in the smart grid," *IEEE Commun. Mag.*, vol. 50, no. 5, pp. 166-172, May 2012.
- [37] B. Qela and H. T. Mouftah, "Observe, learn, and adapt (OLA) VAn algorithm for energy management in smart homes using wireless sensors and artificial intelligence," *IEEE Trans. Smart Grid*, vol. 3, no. 4, pp. 2262-2272, Dec. 2012.
- [38] M. Kantarci and H. T. Mouftah, "Wireless sensor networks for cost-efficient residential energy management in the smart grid," *IEEE Trans. Smart Grid*, vol. 2, no. 2, pp. 314-325, Jun. 2011.
- [39] D. Han and J. Lim, "Design and implementation of smart home energy management systems based on Zigbee," *IEEE Trans. Consumer Electron.*, vol. 56, no. 3, pp. 1417-1425, Aug. 2010.
- [40] Z. Zhu, S. Lambotharan, W. H. Chin, and Z. Fan, "Overview of demand management in smart grid and enabling wireless communication technologies," *IEEE Wireless Commun.*, vol. 19, no. 3, pp. 48-56, Jun. 2012.
- [41] J. Byun, B. Jeon, J. Noh, Y. Kim, and S. Park, "An intelligent self adjusting sensor for smart home services based on Zigbee communications," *IEEE Trans. Consumer Electron.*, vol. 58, no. 3, pp. 794-802, Aug. 2012.
- [42] A. J. D. Rathnayaka, V. M. Potdar, and S. J. Kuruppu, "Evaluation of wireless home automation technologies," in *Proc. IEEE Int. Conf. Digital Ecosyst. Technol.*, Daejeon, Korea, 2011, pp. 76-81.
- [43] A. Hashizume, T. Mizuno, and H. Mineno, "Energy monitoring system using sensor networks in residential houses," in *Proc. IEEE Int. Conf. Adv. Inf. Netw. Appl.*, 2012, pp. 595-600.
- [44] K. Islam, W. Shen, and X. Wang, "Security and privacy considerations for wireless sensor networks in smart home environments," in *Proc. IEEE Int. Conf. Comput. Supported Cooperative Work Design*, 2012, pp. 626-633.
- [45] A. Sleman and R. Moeller, "SOA distributed operating system for managing embedded devices in home and building automation," *IEEE Trans. Consumer Electron.*, vol. 57, no. 2, pp. 945-952, May 2011.
- [46] C. E. P. J. Cordova, B. Asare-Bediako, G. M. A. Vanalme, and W. L. Kling, "Overview and comparison of leading communication standard technologies

- for smart home area networks enabling energy management systems,” *presented at the Int. Conf. Universites Power Eng.*, Soest, Germany, Sep. 5-8, 2011.
- [47] H. Li, S. Gong, L. Lai, Z. Han, R. C. Qiu, and D. Yang, “Efficient and secure wireless communications for advanced metering infrastructure in smart grid,” *IEEE Trans. Smart Grid*, vol. 3, no. 3, pp. 1540-1551, Sep. 2012.
- [48] M. Martinelli, L. Ioriatti, F. Viani, M. Benedetti, and A. Massa, “A WSN-based solution for precision farm purposes,” in *Proc. IEEE Geosci. Remote Sens. Symp.*, Cape Town, South Africa, Jul. 12-17, 2009, vol. 5, pp. 469-472.
- [49] L. Ioriatti, M. Martinelli, F. Viani, M. Benedetti, and A. Massa, “Real-time distributed monitoring of electromagnetic pollution in urban environments,” in *Proc. IEEE Geosci. Remote Sens. Symp.*, Cape Town, South Africa, Jul. 12-17, 2009, vol. 5, pp. 100-103.
- [50] F. Viani, M. Salucci, P. Rocca, G. Oliveri, and A. Massa, “A multi-sensor WSN backbone for museum monitoring and surveillance,” in *Proc. Eur. Conf. Antennas Propag.*, Prague, Czech Republic, 2012, pp. 51-52.
- [51] M. Souryal, C. Gentile, D. Griffith, D. Cypher, and N. Golmie, “A methodology to evaluate wireless technologies for the smart grid,” in *Proc. 1st IEEE Int. Conf. Smart Grid Commun.*, Oct. 2010, pp. 356-361.
- [52] K. Gill, S.-H. Yang, F. Yao, and X. Lu, “A ZigBee-based home automation system,” *IEEE Trans. Consumer Electron.*, vol. 55, no. 2, pp. 422-430, May 2009.
- [53] S. Fang, S. Berber, and A. K. Swain, “Energy consumption evaluations of cluster-based sensor nodes with IEEE 802.15.4 transceiver in flat Rayleigh fading channel,” in *Proc. Int. Conf. Wireless Commun. Signal Process.*, 2009.
- [54] Wireless Medium Access Control (MAC) and Physical Layer (PHY) Specifications for Low-Rate Wireless Personal Area Networks (WPANs), IEEE Std. 802.15.4-2006, 2006.
- [55] ZigBee Alliance, About: The Alliance, 2011. [Online]. Available: <http://www.zigbee.org/About/AboutAlliance/TheAlliance.aspx>.
- [56] T. Lennvall, S. Svensson, and F. Hekland, “A comparison of wireless HART and ZigBee for industrial applications,” *ABB Corporate Res.*, Vasteras, Sweden and Billingstad/Norway, 2008.

BIBLIOGRAPHY

- [57] F. Viani, E. Giarola, F. Robol, G. Oliveri, and A. Massa, "Distributed monitoring for energy consumption optimization in smart buildings," *Proc. 2014 IEEE Antenna Conference on Antenna Measurements and Applications (IEEE CAMA 2014)*, Antibes Juan-les-Pins, France, pp. 1-3, November 16-19, 2014.
- [58] F. Viani, "A decision support system based on wireless power metering for energy saving in smart buildings," *Microwave and Optical Technology Letters*, vol. 57, no. 12, pp. 2750-2752, December 2015.
- [59] A. Mohsenian-Rad, V. W. S. Wong, J. Jatskevich, R. Schober, and A. Leon-Garcia, "Autonomous Demand-Side Management Based on Game-Theoretic Energy Consumption Scheduling for the Future Smart Grid," *IEEE Trans. On Smart Grid*, vol. 1, no. 3, pp. 320-332, Dec. 2010.
- [60] F. Viani, F. Robol, A. Polo, P. Rocca, G. Oliveri, and A. Massa, "Wireless architectures for heterogeneous sensing in smart home applications - concepts and real implementations", *Proc. IEEE*, vol. 101, no. 11, pp. 2381-2396, Nov. 2013.
- [61] A. Massa, A. Boni, and M. Donelli, "A classification approach based on SVM for electromagnetic subsurface sensing," *IEEE Trans. On Geosci. And Remote Sens.*, vol. 43, no. 9, pp. 2084-2094, 2005.
- [62] D. Fudenberg and J. Tirole, *Game Theory*. Cambridge, MA: MIT Press, 1991.
- [63] A.J. Wood and B.F. Wollenberg, *Power generation, operation, and control*, Wiley-Interscience, New York, 1996.
- [64] M.J.D. Powell, A direct search optimization method that models the objective and constraint functions by linear interpolation, In: Gomez and J.-P. Hennart (Eds.), *Advances in optimization and numerical analysis*, Kluwer Academic, Dordrecht, 1994, pp. 51-67.
- [65] F. Viani, A. Polo, P. Garofalo, N. Anselmi, M. Salucci, and E. Giarola, "Evolutionary optimization applied to wireless smart lighting in energy-efficient museums," *IEEE Sensors Journal*, vol. 17, no. 5, pp. 1213-1214, March 2017.
- [66] C. Capurro, D. Nollet, and D. Pletinckx, "Tangible interfaces for digital museum applications," in *Proc. Digital Heritage*, Granada, Spain, Sep./Oct. 2015, pp. 271-276.
- [67] D. W. Boeringer and D. H. Werner, "Particle swarm optimization versus genetic algorithms for phased array synthesis," in *IEEE Transactions on Antennas and Propagation*, vol. 52, no. 3, pp. 771-779, March 2004.

- [68] M. Clerc and J. Kennedy, "The particle swarm - explosion, stability, and convergence in a multidimensional complex space," *in IEEE Transactions on Evolutionary Computation*, vol. 6, no. 1, pp. 58-73, Feb 2002.
- [69] R. C. Eberhart and Y. Shi, "Comparing inertia weights and constriction factors in particle swarm optimization," *Proceedings of the 2000 Congress on Evolutionary Computation.*, La Jolla, CA, 2000, pp. 84-88 vol.1.
- [70] A. I. El-Gallad, M. El-Hawary, A. A. Sallam and A. Kalas, "Swarm intelligence for hybrid cost dispatch problem," *Canadian Conference on Electrical and Computer Engineering 2001. Conference Proceedings*, Toronto, Ont., 2001, pp. 753-757 vol.2.
- [71] E. Ozcan and C. K. Mohan, "Particle swarm optimization: surfing the waves," *Proceedings of the 1999 Congress on Evolutionary Computation-CEC99*, Washington, DC, 1999, pp. 1944 Vol. 3.
- [72] R. Poli, J. Kennedy and T. Blackwell, "Particle swarm optimization - an overview" *Swarm Intell.*, 33-57, 2007.
- [73] Y. Shi and R. Eberhart, "A modified particle swarm optimizer," *IEEE International Conference on Evolutionary Computation Proceedings. IEEE World Congress on Computational Intelligence*, Anchorage, AK, 1998, pp. 69-73.
- [74] Y. Shi and R. C. Eberhart, "Empirical study of particle swarm optimization," *Proceedings of the 1999 Congress on Evolutionary Computation-CEC99*, Washington, DC, 1999, pp. 1950 Vol. 3.
- [75] I. C. Trelea, "The particle swarm optimization algorithm: convergence analysis and parameter selection", *Inform. Process. Lett.*, 2004.
- [76] J. Kennedy and R. Eberhart, "Particle swarm optimization," *Neural Networks, 1995. Proceedings., IEEE International Conference on*, Perth, WA, 1995, pp. 1942-1948 vol.4. (Piscataway, NJ, USA) pp 1942-8
- [77] J. Kennedy, R. C. Eberhart and Y. Shi, "Swarm Intelligence" *San Francisco, CA: Morgan Kaufmann*, 2001.
- [78] Mikki, S. M. and A. A. Kishk, "Physical theory for particle swarm optimization," *Progress In Electromagnetics Research*, Vol. 75, 171-207, 2007.
- [79] J. Robinson and Y. Rahmat-Samii, "Particle swarm optimization in electromagnetics," *in IEEE Transactions on Antennas and Propagation*, vol. 52, no. 2, pp. 397-407, Feb. 2004.

BIBLIOGRAPHY

- [80] F. Viani, F. Robol, E. Giarola, A. Polo, A. Toscano, and A. Massa, "Wireless monitoring of heterogeneous parameters in complex museum scenario," *Proc. 2014 IEEE Antenna Conference on Antenna Measurements and Applications (IEEE CAMA 2014)*, Antibes Juan-les-Pins, France, pp. 1-3, November 16-19, 2014.
- [81] L. De Brito, L. Peralta, F. Santos, and R. Fernandes, "Wireless sensor networks applied to museums environmental monitoring," *IEEE Int. conf. on wireless and mobile commun.*, 2008.
- [82] F. Viani, L. Lizzi, P. Rocca, M. Benedetti, M. Donelli, and A. Massa, "Object tracking through RSSI measurements in wireless sensor networks," *Electron. Lett.*, vol. 44, no. 10, pp. 653-654, May 2008.
- [83] F. Viani, P. Rocca, M. Benedetti, G. Oliveri, and A. Massa, "Electromagnetic passive localization and tracking of moving targets in a WSN infrastructured environment," *Inverse Problems*, vol. 26, pp.15, 2010.
- [84] F. Viani, M. Donelli, P. Rocca, G. Oliveri, D. Trincherro, and A. Massa, "Localization, tracking and imaging of targets in wireless sensor networks," *Radio Science*, vol. 46, no. 5, 2011.
- [85] F. Viani, G. Oliveri, M. Donelli, L. Lizzi, P. Rocca, and A. Massa, "WSN-based solutions for security and surveillance," *40th European Microwave Conference 2010*, Paris, France, September 26 - October 2010.
- [86] F. Viani, M. Martinelli, L. Ioriatti, L. Lizzi, G. Oliveri, P. Rocca, and A. Massa, "Real-time indoor localization and tracking of passive targets by means of wireless sensor networks," *Proc. 2009 IEEE AP-S International Symposium*, Charleston, SC, USA, June 1-5, 2009.
- [87] F. Viani, M. Martinelli, L. Ioriatti, M. Benedetti, and A. Massa, "Passive real-time localization through wireless sensor networks," *Proc. 2009 IEEE International Symposium on Geoscience and Remote Sensing*, Cape Town, South Africa, July 13-17, 2009.
- [88] D. Michie, D. J. Spiegelhalter, and C. C. Taylor, *Machine Learning, Neural and Statistical Classification*. Englewood Cliffs, NJ: PrenticeHall, 1994.
- [89] V. Vapnik, *The Nature of Statistical Learning Theory*. New York: Springer Verlag, 1995.
- [90] A. Massa, G. Oliveri, M. Salucci, N. Anselmi, and P. Rocca, "Learning-by-examples techniques as applied to electromagnetics," *Journal of Electromagnetic Waves and Applications*, Invited Review Article, pp. 1-16, 2017

- [91] T. Evgeniou, M. Pontil, and T. Poggio, "Regularization networks and support vector machines," in *Advances in Large Margin Classifiers*, A. J. Smola, P. L. Bartlett, B. Scholkopf, and D. Schuurmans, Eds, MA: MIT Press, 2000.
- [92] B. Scholkopf and A. Smola, *Learning with Kernels*. Cambridge, MA: MIT Press, 2002.
- [93] Y. Lin, Y. Lee, and G. Wahba, "Support vector machines for classification in nonstandard situations," *Dept. Statistics, Univ. Wisconsin, Madison*, Tech. Rep. 1016, 2000.
- [94] K. Morik, P. Brockhausen, and T. Joachims, "Combining statistical learning with a knowledge-based approach: A case study in intensive care monitoring," *presented at the 16th Int. Conf. Machine Learning*, 1999.
- [95] N. Cristianini and J. Shawe-Taylor, "An Introduction to Support Vector Machines." Cambridge, U.K.: *Cambridge Univ. Press*, 2000.
- [96] V. N. Vapnik, "The Nature of Statistical Learning Theory." New York: *Wiley*, 1999.
- [97] J. Platt, "Fast training of support vector machines using sequential minimal optimization," in *Advances in Kernel Methods-Support Vector Learning*, B. Scholkopf, C. J. C. Burges, and A. J. Smola, Eds. Cambridge, MA: MIT Press, 1999.
- [98] K. R. Muller, S. Mika, G. Ratsch, K. Tsuda, and B. Scholkopf, "An introduction to kernel-based learning algorithms," *IEEE Trans. Neural Netw.*, vol. 12, no. 2, pp. 181-201, Mar. 2001.
- [99] G. Wahba, "Support vector machines, reproducing kernel Hilbert spaces and the randomized GACV," in *Advances in Kernel Methods-Support Vector Learning*, B. Scholkopf, C. J. C. Burges, and A. J. Smola, Eds. Cambridge, MA: MIT Press, 1999.
- [100] T. Hastie and R. Tibshirani. (1996) "Classification by pairwise coupling." Stanford Univ., Stanford, CA. [Online]Tech. Rep.
- [101] J. Platt, "Probabilistic outputs for support vector machines and comparison to regularized likelihood methods," in *Advances in Large Margin Classifiers*, A. J. Smola, P. Bartlett, B. Scholkopf, and D. Schuurmans, Eds. Cambridge, MA: MIT Press, 1999.
- [102] F. Viani, M. Donelli, M. Salucci, P. Rocca, and A. Massa, "Opportunistic exploitation of wireless infrastructures for homeland security," *Proc. 2011 IEEE AP-S International Symposium*, Spokane, USA, July 3-8, 2011.

BIBLIOGRAPHY

- [103] G. Menduni, F. Viani, F. Robol, E. Giarola, A. Polo, G. Oliveri, P. Rocca, and A. Massa, "A WSN-based architecture for the E-Museum - The experience at "Sala dei 500" in Palazzo Vecchio (Florence)," *Proc. 2013 IEEE AP-S International Symposium*, Lake Buena Vista, Florida, USA, pp. 1114-1115, July 7-12, 2013.
- [104] E. Bruns and O. Bimber, "Localization and classification through adaptive pathway analysis," *IEEE Pervasive Computing*, vol. 11, no.2, pp. 74-81, 2012.
- [105] F. Viani, "Opportunistic occupancy estimation in museums through wireless sensor networks," *Microwave and Optical Technology Letters*, vol. 57, no. 8, pp. 1975-1977, August 2015.